



People's Democratic Republic of Algeria
Ministry of Higher Education and Scientific Research
University of Larbi Tebessi –Tebessa



Faculty of Exact Sciences and Sciences of Nature and Life

Department: Matter Sciences

MASTER'S THESIS

Field: Matter Sciences

Discipline: Physics

Option: Condensed Matter Physics

Theme:

*Systematic study of the even-A
Silicon isotopic chain*

Presented by:

RAMDANE Ouahiba

FASSEKH Ghouzlene

Board of Examiners :

Chair :	CHEMAM	Faical	Professor	Larbi Tebessi. Univ Tébessa
Supervisor :	BOUHELAL	Mouna	Professor	Larbi Tebessi. Univ Tébessa
Examiner :	SERDOUK	Fadhila	MCB	Larbi Tebessi. Univ Tébessa

Date of defence : 16/09/2020

Note : 

Mention : *Excellent*



People's Democratic Republic of Algeria
Ministry of Higher Education and Scientific Research
University of Larbi Tebessi –Tebessa



Faculty of Exact Sciences and Sciences of Nature and Life

Department: Matter Sciences

MASTER'S THESIS

Field: Matter Sciences

Discipline: Physics

Option: Condensed Matter Physics

Theme:

*Systematic study of the even-A
Silicon isotopic chain*

Presented by:

RAMDANE Ouahiba

FASSEKH Ghouzlene

Board of Examiners :

Chair :	CHEMAM	Faiçal	Professor	Larbi Tebessi. Univ Tebessa
Supervisor :	BOUHELAL	Mouna	Professor	Larbi Tebessi. Univ Tebessa
Examiner :	SERDOUK	Fadhila	MCB	Larbi Tebessi. Univ Tebessa

Date of defence : 16/09/2020

Note :

Mention :



Déclaration sur l'honneur de non-Plagiat

(À joindre obligatoirement au mémoire; Remplie et signée)

Nous soussignons

Nom, prénom: **FASSEKH Ghaylene & RAMDHANE Ouadloua**

N° de carte d'étudiant: (1) **201534030064** (2) **201534021500**

Régulièrement inscrits (es) en **Master** au **Département Sciences de la Matière**

Année universitaire: **2019/2020**

Domaine: **Sciences de la matière**

Filière: **Physique**

Spécialité: **Physique de matière condensée**

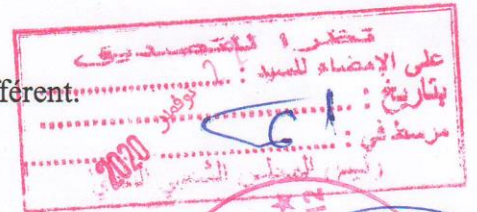
Intitulé du mémoire: **Systematic study of the even-A Silicon isotopic chain.**

Attestons que notre mémoire est un travail original et que toutes les sources utilisées ont été indiquées dans leur totalité. Nous certifions également que nous n'avons ni recopié ni utilisé des idées ou des formulations tirées d'un ouvrage, article, ou mémoire, en version imprimée ou électronique, sans mentionner précisément leur origine et que les citations intégrales sont signalées entre guillemets.

Sanctions en cas de plagiat prouvé:

Les étudiants seront convoqués devant le conseil de discipline, les sanctions prévues selon la gravité du plagiat sont:

- L'annulation du mémoire avec possibilité de le refaire sur un sujet différent.
- L'exclusion d'une année du master.
- L'exclusions définitive.

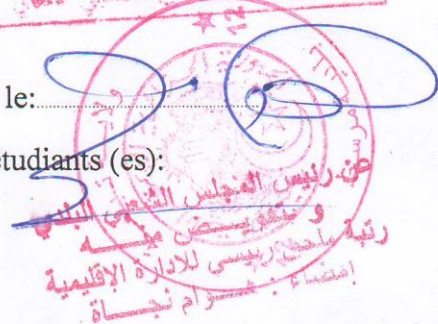


Fait à Tébessa, le:

Signature des étudiants (es):

(1):

(2):



Thesis achieved

At

Laboratoire de Physique Appliquée et Théorique LPAT



Abstract

We are interested in our work to the sd shell nuclei whose energy spectra contain, at low excitation energies, positive- and negative- parity states.

The normal positive parity states are well described using the well-known interactions (USD and USDA/B) within the sd shell valence space. The intruder negative parity states require the extension of the valence space to the full p-sd-pf. A PSDPF interaction was built to describe, simultaneously, both types of states coexisting in the sd shell nuclei using a fitting procedure. As the states of the middle of sd-shell nuclei could not be fitted, due to computational limitations, we decided to study a set of those nuclei, which are the silicon isotopic chain.

In this work, we will systematically study the excitation energy evolutions for first excited positive- and negative-parity states in the even-A silicon isotopic chain using the PSDPF interaction. A detailed discussion of the obtained results will be presented.

Résumé

Nous sommes intéressés dans notre travail aux noyaux de la couche sd dont les spectres en énergie contiennent, à basses énergies d'excitation, des états de parité- positive et négative.

Les états normaux de parité positive sont bien décrits en utilisant les interactions bien connues (USD et USDA/B) dans l'espace de valence de la couche sd. Les états intrus de parité négative nécessitent l'extension de l'espace de valence à l'espace p-sd-pf complet. Une interaction PSDPF a été construite pour décrire, simultanément, les deux types d'états coexistant dans les noyaux de la couche sd en utilisant une procédure d'ajustement. Comme les états des noyaux du milieu de la couche sd n'ont pas pu être ajustés, en raison de limitations informatiques, nous avons décidé d'étudier un ensemble de ces noyaux, qui sont la chaîne isotopique du silicium.

Dans ce travail, nous étudierons systématiquement l'évolution des énergies d'excitation pour les premiers excités états de parité- positive et négative dans la chaîne isotopique du silicium avec A-pair en utilisant l'interaction PSDPF. Une discussion détaillée des résultats obtenus sera présentée.

ملخص

نحن مهتمون في عملنا بأنوية طبقة ال sd، التي أطياف طاقتها تحوي، عند طاقات الإثارة المنخفضة، على حالات ذات زوجية- موجبة وسالبة.

تم وصف الحالات العادية ذات الزوجية الموجبة باستخدام التفاعلات المعروفة جيدا (USD,USDA/B) في فضاء التكافؤ لطبقة ال sd. تتطلب الحالات الدخيلة ذات الزوجية السالبة تمديد فضاء التكافؤ إلى الفضاء الكامل p-sd-pf. تم إنشاء تفاعل PSDPF لوصف، في وقت واحد، النوعين من الحالات التي تتعايش في نوى طبقة sd باستخدام طريقة التعديل. بما أن حالات أنوية منتصف الطبقة sd لا يمكن تعديلها، بسبب القيود الحسابية، فقد قررنا دراسة مجموعة هذه الأنوية، وهي سلسلة نظائر السيليكون.

في هذا العمل، سوف ندرس بشكل منهجي تطور طاقات الإثارة للحالات المثارة الموجبة و السالبة الأولى في السلسلة النظائرية ذات A زوجي للسيليكون باستخدام تفاعل PSDPF. سيتم تقديم مناقشة مفصلة للنتائج التي تم الحصول عليها.

Ghozlene's Dedication

Every challenging work needs self-efforts as well as guidance of elders especially those who were very close to our heart. First, Thank God for helping me achieve this, than I want to thank myself for its steadfastness to this moment, and I hope that this is the first step in the journey to achieve the goal.

My humble effort I dedicate to my sweet and loving Father Mohamed and Mother Laarem whose affection, love, encouragement and prays of days and night make me able to get such success and honor. May God protect you and heal you and prolong your life

To my dear sister Zainab and her husband and the lover of his aunt Qais, to both Rawiya and Omaima's twins, to my dear brother Zakaria, No dedication can express all the love I have for you, Your joy and your gaiety fill me with happiness. May God keep you, light your way and help you realize your dearest wishes.

To my grandmother, who has accompanied me with his prayers, his gentleness, may God lend him long life and a lot of health and happiness in lives, my uncles, my aunts. Especially my aunt Kamla and my uncle Wahide and his wife Samia, Thank you for your support, I express my sincere love and respect for you.

To my dear best and my intimate friend Hadjer, In remembrance of our sincere and deep friendship and of the moments pleasant that we spent together.

To my dear, my partner Ouahiba , to whom I wish all the happiness and success of the world, god protect you and thank you for being my friend.

All thanks to my distinguished teacher, BOUHLAL Mouna, who believed in me, encouraged me and supported me for the last minute of our work.

To every person I have met in my life who has helped me even with a kind word, especially someone who has supported me in all my challenges, thank you for everything.

Fassech Ghozlene

Ouahiba's Dedication

First of all, thank God, I have successfully completed this work, i start my dedication to my future self... Hello! I hope that you have achieved all that you have hoped and aimed at, and from all my heart i dedicate this work to all who wished and eagerly waited for my discussion of this thesis, but the Coronavirus pandemic was on the lookout! Really, 2020 is unforgettable. I dedicate this humble work to my parents. One of the proudest names I hold is my dear father “Mohamed”, who has always believed in me and praised me, also my mother “Fadhila”; who waited for my completion of my studies to see me as a successful and mature daughter. To my dear sister “Nada eraihane” and my brothers” Nour el islem” and “Taha” and my dear little one “Moez billeh”... Your older sister has done it and graduated. To my big family, especially my grandmother “may god have mercy on her soul”, who so sad because of the come across for the global epidemic with my graduation, to my dear friends, I love you very much and thank you very much one by one... To everyone who cares about me. To every teacher who taught me a letter throughout my courses .And so much love to my supervisor “ BOUHELAL Mouna”, who believed in me and supported me in the challenge I chose in the subject of this thesis to prove that you would not be a true physicist if you had only specialized in one field... to my partner in this work “Ghozlene” , I’m sorry for every time i lost my temper. I really enjoyed this achievement with you.

To all who knew me and to all those who did not know me yet, I dedicate this humble work to you.

Ouahiba Ramdane

Acknowledgments

To our Supervisor,

PROFESSOR BOUHELAL Mouna

We thank you for the kindness and spontaneity with which you were kind enough to direct this work. We have had the great pleasure of working under your direction, You were a competent advisor and guide. Your indisputable professional competences as well as your human qualities earn you the admiration and respect of all.

*We thank *Dr. SERDOUK Fadhila* and *PROF. CHEMAM Faïçal* for the honour they did in chairing the jury of our thesis, it is a great honor for us to see you sit on our jury. We are very grateful for the spontaneity and the kindness with which you agreed to judge our work.*

you will find in this modest work the expression for our high consideration, our sincere gratitude and our deep respect.

We extend our thanks to all my teachers who gave us a scientific basis.

Our thanks to all those who have helped us in our journey and to our distinguished professors and to all employees of the administration .

Ouahiba & Ghoulene

Table of Contents:

<i>Abstract</i>	I
<i>Résumé</i>	II
<i>ملخص</i>	III
<i>Ghozlene's dedication</i>	IV
<i>Ouahiba's dedication</i>	V
<i>Acknowledgments</i>	VI
<i>Table of contents</i>	VII
<i>List of Tables</i>	IX
<i>List of Figures</i>	XI
<i>List of Symbols</i>	XIV
<i>Introduction</i>	1
<i>Chapter I: The nuclear shell model</i>	2
1. Magic nuclei	2
1.1 <i>The special features of magic nuclei</i>	2
2. Shell model	5
3. Independent particle model	5
3.1 <i>The harmonic oscillator potential</i>	5
3.2 <i>The spin-orbit interaction</i>	9
3.2 <i>The nucleon-nucleon interaction</i>	11
4. Beyond the mean field	11
5. Ingredients of the shell model	12
5.1 <i>The Choice of the Valence Space</i>	12
5.2 <i>Effective interaction</i>	13
5.3 <i>The computational code</i>	14
<i>Chapter II: The sd-shell nuclei</i>	15
1. The spherical normal states	16
2. The intruder states	16
2.1 <i>The intruder spherical negative parity state states</i>	16
3.2 <i>The positive and negative parity intruder state</i>	17
3. The PSDPF interaction	17
3.1 <i>The construction of the PSDPF interaction</i>	18
3.2 <i>Shell model ingredients in case of sd-shell nuclei</i>	18
4. Application of the shell model	18
4.1 <i>Parity</i>	18
4.2 <i>Nuclear spin</i>	18

4.3 <i>Isospin</i>	19
4.4 <i>Shell occupation</i>	20
5. Nucleons distribution	22
Chapter III: Systematic study of the even-A Silicon isotopic chain	28
1. Properties of the Silicon element	28
1.1 <i>Interesting facts</i>	28
1.2 <i>Physical properties</i>	28
2. Properties of Silicon isotopes	29
2.1 <i>The even-A Silicon isotopes</i>	29
2.2 <i>Experimental review of excitation energies in even-A Silicon isotopes</i>	31
3. Systematics of the even-A Silicon isotopic chain study	39
3.1 <i>comparison calculated versus experimental excitation energies of the test states</i>	39
3.2 <i>systematics of the excitation energies of the test states in even-A silicon isotopes</i>	44
General conclusion	56
Bibliographic references	57
Appendix -A	59
Appendix -B	60

List of Tables

<u>Table N°</u>	<u>Title</u>	<u>Page</u>
<u>Table I-1</u>	Binding energy of nuclei with $15 \leq A \leq 17$ [8].	3
<u>Table II-1</u>	Calculation of the probability for the different configuration (shell occupation probabilities) given rise the first excited state 2^+ .	26
<u>Table II-2</u>	Calculation of the probability for the different configuration (shell occupation probabilities) given rise the first excited state 3^- .	27
<u>Table III-1</u>	Comparison of properties of excited states in Si^{22} and its mirror nucleus [8].	31
<u>Table III-2</u>	Comparison of properties of excited states in Si^{24} and its mirror nucleus [8].	32
<u>Table III-3</u>	Comparison of properties of excited states in Si^{26} and its mirror nucleus [8].	33
<u>Table III-4</u>	Experimental review of excitation energies in Si^{28} [8].	35
<u>Table III-5</u>	Experimental review of excitation energies in Si^{30} [8].	36
<u>Table III-6</u>	Experimental review of excitation energies in Si^{32} [8].	37
<u>Table III-7</u>	Experimental review of excitation energies in Si^{34} [8].	38
<u>Table III-8</u>	Calculated excitation energies (in MeV) of the test states even-A silicon isotopes.	39
<u>Table III-9</u>	The energy excitation calculation by adding the rmsd.	42

List of Figures

<u>Figure N^o</u>	<u>Title</u>	<u>Page</u>
<u>Figure I-1</u>	The binding energy of nuclei per nucleons [7].	3
<u>Figure I-2</u>	The binding energy [8] of the nuclei with $15 \leq A \leq 17$.	4
<u>Figure I-3</u>	Schematic of the harmonic oscillator potential major shells whose energy degeneration is given by G_n .	6
<u>Figure I-4</u>	Difference between the wood-Saxon potential and the harmonic oscillator potential [13].	7
<u>Figure I-5</u>	Diagram of the shell model using the potential $V_{HO} - Dl^2$.	8
<u>Figure I-6</u>	The degeneration of states n, l .	9
<u>Figure I-7</u>	Diagram of the shell model single-particle orbitals [15].	10
<u>Figure I-8</u>	Diagram of the valence space.	13
<u>Figure II-1</u>	Chart of sd shell nuclei [8]. For the nuclei selected with a star «*» the ground state is unbound, i.e. unstable compared to particle emission.	15
<u>Figure II-2</u>	Chart of sd nuclei with known negative parity intruder states [8].	17
<u>Figure II-3</u>	Different nucleon distributions that gives the ground states J^Π values in some nuclei.	19
<u>Figure II-4</u>	Wave-particle duality [35].	22
<u>Figure II-5</u>	Distribution of nucleons forming the ground state of ^{26}Si .	23
<u>Figure II-6</u>	Schematic of the configuration of the first excited states 2^+ and 3^- of the ^{26}Si .	24
<u>Figure III-1</u>	The atomic model of the Silicon atom.	29
<u>Figure III-2</u>	Comparison between the experimental and calculated excitation energies of the state 2^+ in even-A Silicon isotopes	40

<u>Figure III-3</u>	Comparison between the experimental and calculated excitation energies of the 3^+ in even-A Silicon isotopes.	40
<u>Figure III-4</u>	Comparison between the experimental and calculated excitation energies of the 4^+ in even-A Silicon isotopes.	41
<u>Figure III-5</u>	Comparison between the experimental and calculated excitation energies of the 1^- in even-A Silicon isotopes.	41
<u>Figure III-6</u>	The new comparison between the experimental and calculated excitation energies of the 1^- in even-A silicon isotopes.	42
<u>Figure III-7</u>	Comparison between the experimental and calculated excitation energies of the 3^- in even-A Silicon isotopes.	43
<u>Figure III-8</u>	Comparison between the experimental and calculated excitation energies of the 4^- in even-A Silicon isotopes.	43
<u>Figure III-9</u>	Comparison between the experimental and calculated excitation energies of the 5^- in even-A Silicon isotopes.	44
<u>Figure III-10</u>	Shell occupation probabilities of the 2^+ state.	48
<u>Figure III-11</u>	Shell occupation probabilities of the 3^+ state.	49
<u>Figure III-12</u>	Shell occupation probabilities of the 4^+ state.	50
<u>Figure III-13</u>	Shell occupation probabilities of the 1^- state.	51
<u>Figure III-14</u>	Shell occupation probabilities of the 3^- state.	52
<u>Figure III-15</u>	Shell occupation probabilities of the 4^- state.	53
<u>Figure III-16</u>	Shell occupation probabilities of the 5^- state.	54

List of symbols

$V(\mathbf{r})$	The Woods-saxon potential.
V_{HO}	Harmonic-oscillator potential.
R_0	the radius of the nucleus.
r_0	The reduced radius.
a	The diffusivity.
V_0	The depth.
M	The mass of a nucleon.
ω	The harmonic-oscillator frequency.
ϵ	The harmonic-oscillator energy.
h_i	The Hamiltonian of an individual nucleon.
T_i	Kinetic energy of nucleon i .
V_{ij}	two-body interaction between the nucleons i and j .
H_0	the independent movement of nucleons in the nucleus.
H_r	The residual interaction.
USDA	sd shell universal interaction compatible with sd valence space (updated version of the USD interaction).
USDB	sd shell universal interaction for compatible with sd valence space (updated version of the USD interaction).
USD	sd shell universal interaction compatible with sd valence space.
Z	Protons number.
N	Neutrons number.
A	Nucleons number.
PSDPF	Effective interaction for sd shell nuclei compatible with p-sd-pf valence space.
π	Proton.
ν	Neutron.
Π	Parity.
$0h\omega$	State of positive parity (0 particle-0 hole jump).
$1h\omega$	State of negative parity (1 particle-1 hole jump).

General introduction

Nuclear structure physics has been evolving to adapt to the growing knowledge of the nuclear landscape since the conception of an atomic nuclear core by Rutherford's early 1900s scattering experiments [1]. Afterwards, the consideration of the proton, as a fundamental particle, was exposed by Rutherford in 1919 [2]. However, it was not until the work of Chadwick in 1932 [3], that the existence of the neutron as a fundamental particle was also discovered.

Nowadays, we have a good understanding of the properties of the structure of the nucleus; containing two types of particles: protons and neutrons. It is clear that experimental and theoretical studies in nuclear physics have played a notable part in the development of twentieth-century physics.

The understanding of the nuclei's properties such as nuclear masses, energy spectra, wave functions, electromagnetic transitions, and nucleon density distributions is always the key problem. Therefore, several models have been developed to solve these problems; among them is the nuclear shell model, which is often referred to as the *naive shell model* or the *independent particle shell model*.

The sd shell nuclei, whose number of protons (Z) and of neutrons (N) between 8 and 20. This area is one of the most studied regions using state-of-the-art shell model. The structure of those nuclei has been the subject of renewed interest in recent years [4]. These nuclei are characterized by the coexistence, at low excitation energies, of normal positive parity states, called also $0\hbar\omega$ states, and intruder negative parity states called also $1\hbar\omega$ states. These two kinds of states are described by the PSDPF interaction, developed by M. BOUHELAL et al., using a fitting procedure. This interaction describes quite well the intruder negative parity states of nuclei at the beginning of the sd shell around ^{16}O and at the end of the sd shell near ^{40}Ca , which were included in the fit. During the fit, states belonging to nuclei of the middle of the sd shell could not be adjusted, we decided thus to study such states in an isotopic chain.

We used the PSDPF [5,6] interaction to make a systematic study about the evolution of the excitation energies of the first positive- and negative- parity states in the even-A isotopes of silicon: ^{22}Si , ^{24}Si , ^{26}Si , ^{28}Si , ^{30}Si , ^{32}Si , ^{34}Si . The calculations were performed using the shell model code Nathan, developed by E. Caurier in the IPHC theoretical physics group. The obtained results will be compared to available experimental data.

In this sense, our thesis contains three fundamental chapters distributed as follows:

- ✚ **Chapter I:** provides an overview of the development of the nuclear shell model, its basics, and how it simplifies the understanding of the nuclear structure.
- ✚ **Chapter II:** introduces the properties of the sd shell nuclei and the PSDPF interaction.
- ✚ **Chapter III:** exposes a detailed discussion of the obtained results and a systematic study of the even-A silicon isotopic chain first excited states.

This dissertation ends with a general conclusion.

Chapter I

The Nuclear Shell Model

The Liquid Drop Model, which examines the global properties of nuclei, underestimated the binding energies of “magic nuclei” for which either the number of neutrons N or the number of protons Z is equal to one of the following “magic numbers” 2, 8, 20, 28, 50, 82, 126. The nuclear shell model was first proposed by Bartlett in 1932 and further developed in 1949 independently by several physicists such as Maria Goeppert–Mayer [7] (following a remark of Fermi) as well as Hans Jensen and H.E Sues [8], and independently by D. Haxel who shared the Nobel Prize in Physics in 1963 with Eugène Wigner for this work.



Maria Goeppert-Mayer



J. Hans D. Jensen



1963 Nobel Prize in Physics

The aim of this chapter and our work is to understand how this model offers the possibility of exploring different properties of nuclei (such nuclear systematics and the internal structure of the nucleus), in particular the stability of **magic nuclei**.

1. Magic nuclei

A magic nucleus has a proton number Z or a neutron number N equals to 2, 8, 20, 28, 50, 82 and 126 known as “magic numbers”. Such nucleus has a higher average binding energy per nucleon than one would expect based upon predictions like the Liquid Drop Model and hence, it is more stable against nuclear decay and then its nearby nuclei.

Nuclei, which have both neutron number and proton number equal to one of the magic numbers, can be called “**doubly magic**“, and are found to be particularly stable.

1.1 Special features of magic nuclei

✓ The strong indication of the magic numbers is the stability of these nuclei. All the stable elements at the end of the natural radioactive series have a magic N or a magic Z or both. We mention a few examples:

- ◆ **Stable magic nuclei:** ${}^{18}_8\text{O}_{10}$, ${}^{44}_{20}\text{Ca}_{24}$, ${}^{60}_{28}\text{Ni}_{32}$, ${}^{114}_{50}\text{Sn}_{64}$.
- ◆ **Stable doubly magic nuclei:** ${}^4_2\text{He}_2$, ${}^{16}_8\text{O}_8$, ${}^{40}_{20}\text{Ca}_{20}$, ${}^{208}_{82}\text{Pb}_{126}$.

There are more stable isotopes, nuclei with same Z , if Z is a magic number, and more stable isotones, nuclei with same N , if N is a magic number.

✓ The neutron (proton) separation energies of such magic nuclei are higher than those of their neighbours.

✓ The binding energy of magic nuclei is much larger than the nearby nuclei as shown on Fig. I-1.

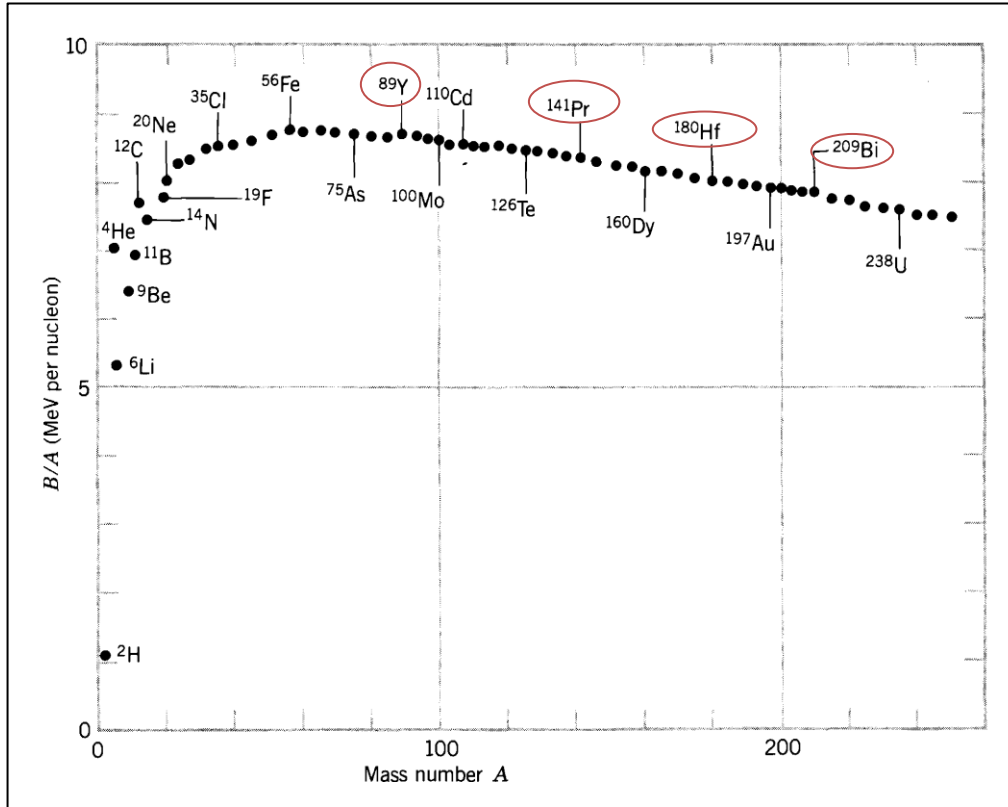


Figure I -1: The binding energy of nuclei per nucleon [9]. The circled elements have a magic number of N or Z .

To illustrate the differences in binding energies in nearby nuclei, we take example of nuclei with nucleon number between $15 \leq A \leq 17$, their binding energies are presented on Table I-1 and on Fig I-2.

${}^A_Z X_N$	${}^{15}_4 Be_{11}$	${}^{15}_5 B_{10}$	${}^{15}_6 C_9$	${}^{15}_7 N_8$	${}^{16}_4 Be_{12}$	${}^{16}_5 B_{11}$	${}^{16}_6 C_{10}$	${}^{16}_8 O_8$
Binding energy (keV)	4541	5880	7100	7699.46	4285	5507.3	6922.05	7976.21
	${}^{17}_{10} Ne_7$	${}^{17}_6 C_{11}$	${}^{17}_5 B_{12}$	${}^{17}_9 F_8$				
	6640.50	6558	5270	7542.33				

Table I-1: Binding energy of nuclei with $15 \leq A \leq 17$ [10]. Magic and doubly magic are highlighted in yellow.

N.B: we can see that the binding energy of the magic nuclei is larger than their nearby ones and the largest binding energy is found for the doubly magic nucleus $^{16}_8\text{O}_8$.

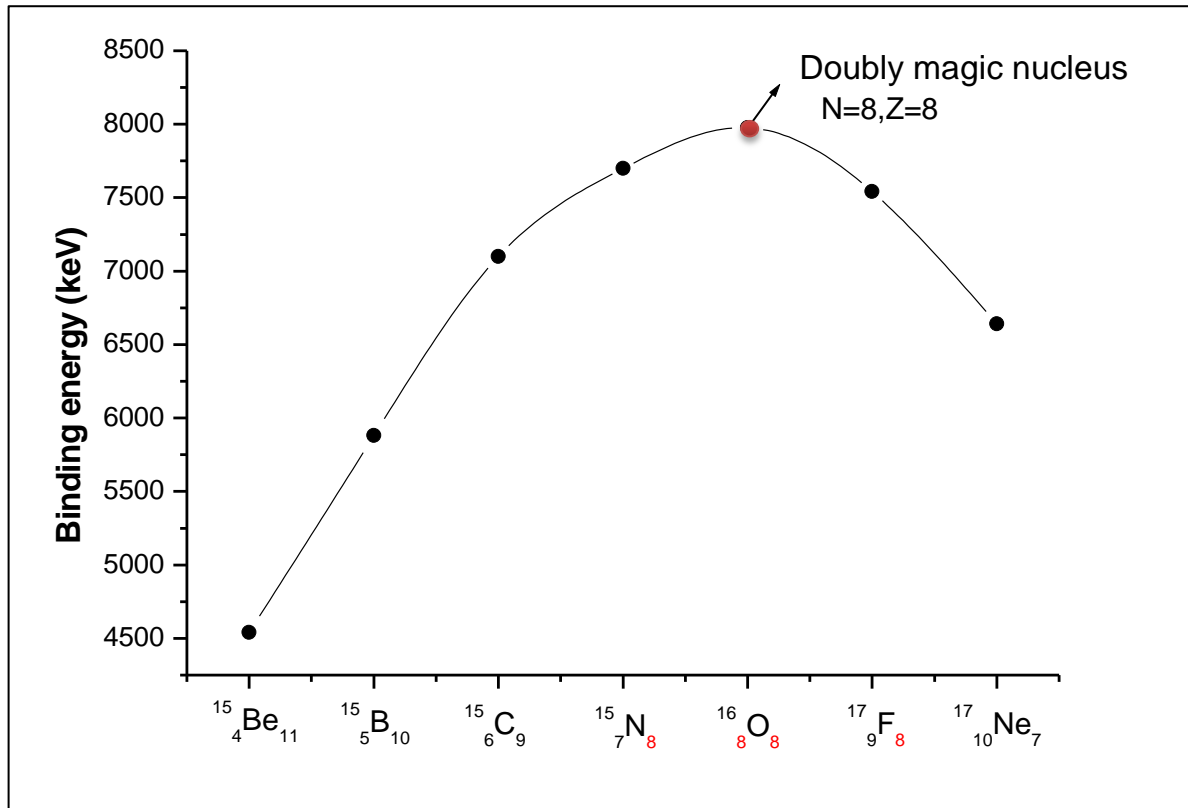


Figure I-2: Binding energy [10] of nuclei with $15 \leq A \leq 17$.

- ✓ Magic number nuclei have higher first excitation energy.
- ✓ There are more *stable isotopes (isotones)* if Z (N) is a magic number. We take as an example the stable Tin isotopes:
 - * $^{112}_{50}\text{Sn}$, $^{114}_{50}\text{Sn}$, $^{115}_{50}\text{Sn}$, $^{116}_{50}\text{Sn}$, $^{117}_{50}\text{Sn}$, $^{118}_{50}\text{Sn}$, $^{119}_{50}\text{Sn}$, $^{120}_{50}\text{Sn}$, $^{122}_{50}\text{Sn}$, $^{124}_{50}\text{Sn}$.
- For the sd shell, region of our interest, the stable isotopes for Oxygen and Calcium nuclei are:
 - * Oxygen: $^{16}_8\text{O}$, $^{17}_8\text{O}$, $^{18}_8\text{O}$.
 - * Calcium: $^{40}_{20}\text{Ca}$, $^{42}_{20}\text{Ca}$, $^{43}_{20}\text{Ca}$, $^{44}_{20}\text{Ca}$, $^{46}_{20}\text{Ca}$.
- ✓ Nuclides with a magic number of neutrons are observed to have a relatively low probability of absorbing an extra neutron, i.e. they have the lowest cross section for neutron absorption (neutron-capture cross sections).

These magic numbers can be explained in terms of the **Nuclear Shell Model**.

2. Shell Model

The nuclear shell model has two essential features: first, the identification of the shell structure itself, based on the evidence for nuclear stability (magic nuclei mentioned earlier) and leading to the basic assumption that the nucleus can be described by a *Single Particle Model*. Second, the assumption of the strong spin-orbit interaction between nucleons that explains the splitting of their energy levels [11].

3. Independent particle model

The *Independent Particle Model* can be applied to complicated systems of identical particles to determine their ground state and the first excited states. It has been used with real success so far only for atoms [12]. The main idea of this model is that a nucleon moves inside a certain potential well (which keeps it bound to the nucleus) independently from the other nucleons. This amounts to replace an N -body problem (N particles interacting) by N single-body problems. One of the most used central potential is **the harmonic oscillator**, which will be discussed, in the next part.

3.1 The harmonic oscillator potential

It is assumed that the interaction between one nucleon and the $(A-1)$ nucleons, in the nucleus, can be approached to a central potential like the harmonic-oscillator potential which can be written as [13]:

$$V_{HO} = \frac{1}{2}m_0\omega^2r^2 \quad (I - 1)$$

Where ω is the frequency of oscillation of the particle with mass m_0 , r is the distance between the nucleon and the origin.

The Schrödinger equation for the nucleons in the harmonic oscillator potential takes the form:

$$H_0\Phi = E_0\Phi \quad (I - 2)$$

H_0 is the Hamiltonian of the independent particles which can be written as:

$$H_0 = \sum_i^A h_{i0} \rightarrow E_0 = \sum_i^A \epsilon_{i0} \quad (I - 3)$$

h_{i0} is single-particle Hamiltonian:

$$h_{i0} = t_i + \frac{1}{2}m\omega^2r^2 \quad (I - 4)$$

We note that, for any spherically symmetric potential well $V(r)$, the eigenvalues and eigenfunctions of the single-particle Hamiltonian, issued from the harmonic-oscillator potential, have the form:

$$\phi_i(r) = \phi_{\tilde{n}lm_l m_s}(r, \theta, \varphi) = R_{\tilde{n}}(r) Y_l^{m_l}(\theta, \varphi) \chi_{m_s}(s) \quad (I - 5)$$

$$\varepsilon = \hbar\omega \left(2\tilde{n} + l + \frac{3}{2} \right), \quad \tilde{n} = 0, 1, 2, \dots \quad (I - 6)$$

We pose: $\tilde{n} = (n-1)$

$$\Rightarrow \varepsilon = \hbar\omega \left(2(n-1) + l + \frac{3}{2} \right) = \hbar\omega \left(N + \frac{3}{2} \right) \quad (I - 7)$$

The constant $\hbar\omega$ of the harmonic oscillator potential is found to be: $\hbar\omega = 41A^{-1/3}\text{MeV}$

(e.g., $\hbar\omega \approx 8\text{MeV}$ for medium and heavy nuclei)

$$\Rightarrow \phi_{nlm_l m_s}(r, \theta, \varphi) = R_n(r) Y_l^{m_l}(\theta, \varphi) \chi_{m_s}(s) \quad (I - 8)$$

Here l and m_l are the quantum numbers of angular momentum and its projection, respectively, while n is the radial quantum number. Note that the quantum orbitals are represented by the symbols s, p, d, f, g, ... corresponding to $l=0, 1, 2, 3, 4, \dots$, respectively.

N denotes the major oscillator quantum number that determines the major shells of the harmonic oscillator potential defined as: $N = 2(n-1)+l$.

Unfortunately, using the harmonic oscillator potential we obtain, as shown on Fig. I-3, only the first three magic numbers: 2, 8, 20.

$5\hbar\omega$	<u>3p</u>	<u>2f</u>	<u>1h</u>	42	112
$4\hbar\omega$	<u>3s</u>	<u>2d</u>	<u>1g</u>	30	70
$3\hbar\omega$	<u>2p</u>	<u>1f</u>		20	40
$2\hbar\omega$	<u>2s</u>	<u>1d</u>		12	20
$1\hbar\omega$	<u>1p</u>			6	8
$0\hbar\omega$	<u>1s</u>			2	2
$N\hbar\omega$	n, l			G_N	$\sum G_N$
				$G_N = (N+1)(N+2)$	

Figure I-3: Schematic of the harmonic oscillator potential major shells whose energy degeneration is given by G_N .

The degeneration in l is an accidental degeneration resulting from V_{HO} potential that does not appear using another central potential such as the Wood-Saxon potential well [14]. To deal with this problem we apply the so-called «the edge effect» in order to remove partially this

degeneration in l by simulating the harmonic oscillator potential to Wood-Saxon well, see Fig. I-4, as following:

$$V_{WS} = V_{HO} + (V_{WS} - V_{HO}) = V_{HO} + \Delta V \quad (I - 9)$$

Where: the Wood-Saxon potential is an example of a mean field central potential (it's details adjusted using experimental observations) was parameterized in 1954 by R. Woods and D. Saxon [14], this admits that the shape of the potential is the same as that of the Fermi distribution, and the same also as the nuclear density, its formula is given by:

$$V_{WS}(r) = \frac{V_0}{1 + e^{\left(\frac{r-R_0}{a}\right)}} \quad (I - 10)$$

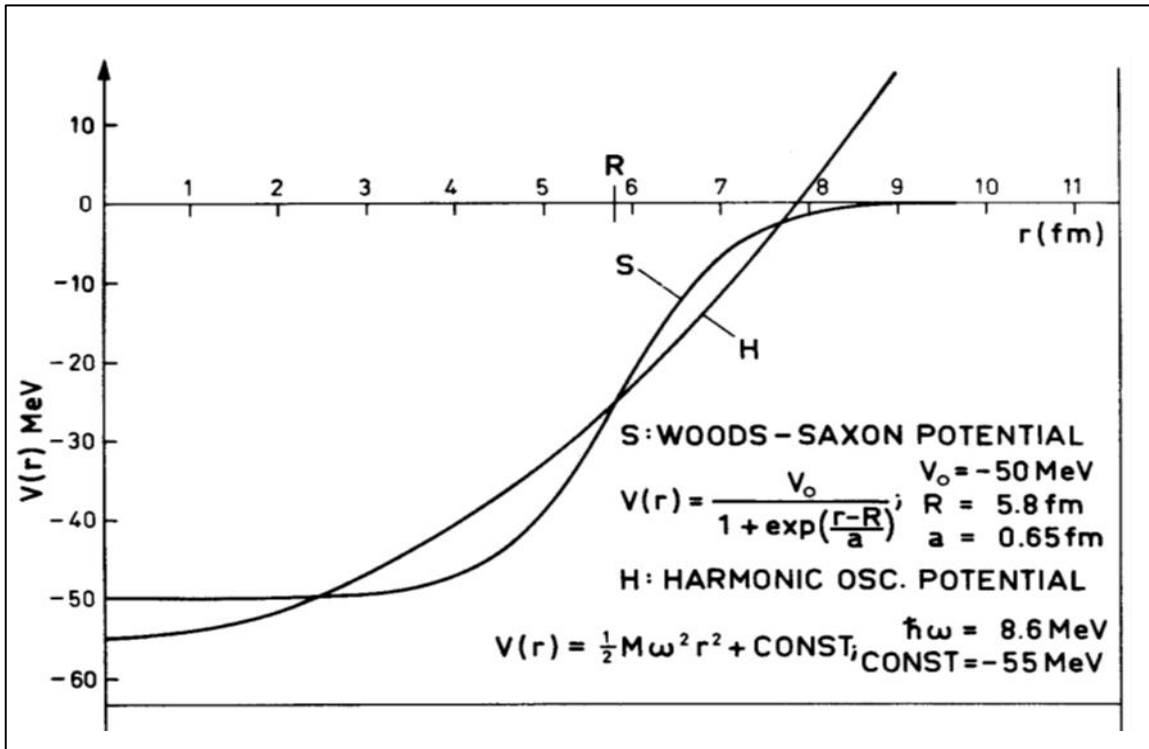


Figure I-4: Difference between the wood-Saxon potential and the harmonic oscillator potential [15].

The simulation between the Wood-Saxon and harmonic oscillator potentials is given by the expression [14]:

$$V_{WS} \approx V_{HO} - D l^2 \quad (I - 11)$$

Where D is a positive parameter adjusted to reproduce the reduction $-D(l+1)$ of the observed states, with the condition of $-D l^2 \ll V_{HO}$ to consider the «the edge effect» as a perturbation of the main potential V_{HO} . This corrective term of type $-D l^2$ has been added to the main previous Hamiltonian as:

$$h_{i0} = t_i + \frac{1}{2} m \omega^2 r^2 - D l^2 \quad (I - 12)$$

The solution of the Schrödinger equation using the new Hamiltonian, in the theory of perturbation, gives the eigenenergy as:

$$\epsilon_{nl}^i = \hbar\omega \left(N + \frac{3}{2} \right) - D l(l+1)\hbar^2 \quad (I - 13)$$

In this case, the energy is related to the quantum numbers n and l , as in Wood-Saxon potential. The degeneration on l is partially removed but only the first three magic numbers 2, 8, 20 were obtained, see Fig I-5.

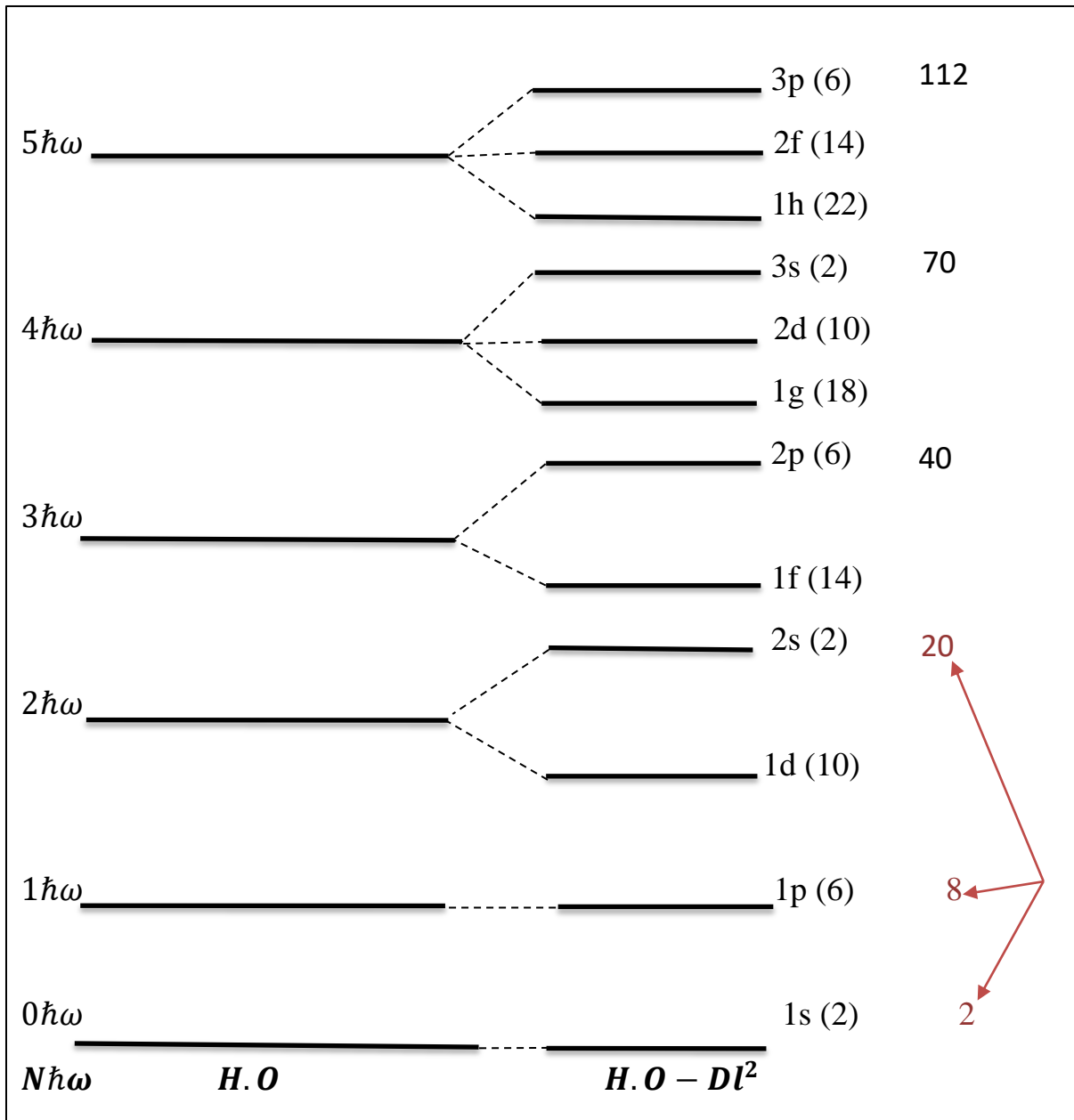


Figure I-5: Diagram of the shell model using the potential V_{HO-Dl^2} .

3.2 The spin-orbit interaction

It was pointed out (independently by Mayer (1949, 1950) and Haxel, Jensen and Suess (1949, 1950)) that a contribution to the average field felt by each individual nucleon should contain a spin-orbit term [16].

The single-particle Hamiltonian becomes thus:

$$h_i = t_i + \frac{1}{2}m\omega^2 r_i^2 + Dl^2_i + f(r)\vec{l}_i\vec{S}_i \quad (I - 14)$$

The corresponding eigenfunctions have the following form:

$$\phi_{nljm}^i(r, \sigma) = R_{nl}(r) \sum_{m_l, m_s} \langle lm_l \frac{1}{2} m_s | jm \rangle Y_l^{m_l}(\theta, \varphi) \chi_s^{m_s} \sigma \quad (I - 15)$$

$$\text{with } m = m_l + m_s$$

The corresponding eigenvalues, now become:

$$E_{nlj}^i = \left(N + \frac{3}{2}\right) \hbar\omega + Dl(l+1)\hbar^2 + \frac{\hbar^2}{2} \langle f(r) \rangle_{nl} \begin{cases} -(l+1) & j = l - \frac{1}{2} \\ l & j = l + \frac{1}{2} \end{cases} \quad (I - 16)$$

The radial function $\langle f(r) \rangle$ is negative, which means that the states with $j = l + \frac{1}{2}$ are always lower in energy than the states with $j = l - \frac{1}{2}$; as shown on the Fig I-6.

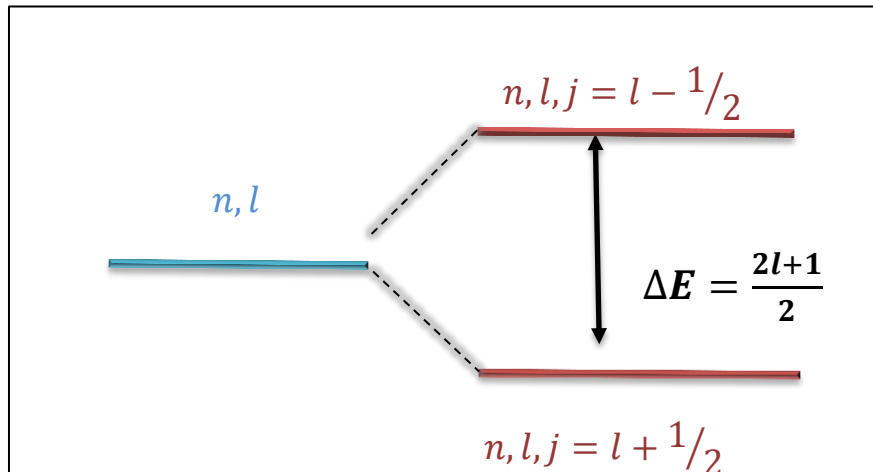


Figure I-6: The degeneration of states with n, l .

The spin-orbit interaction leads to all the magic numbers 2, 20, 28, 50, 82 and 126. The schematic representation of the single-particle energies (individual orbitals) including the three previous potential terms is shown in the Fig I-7.

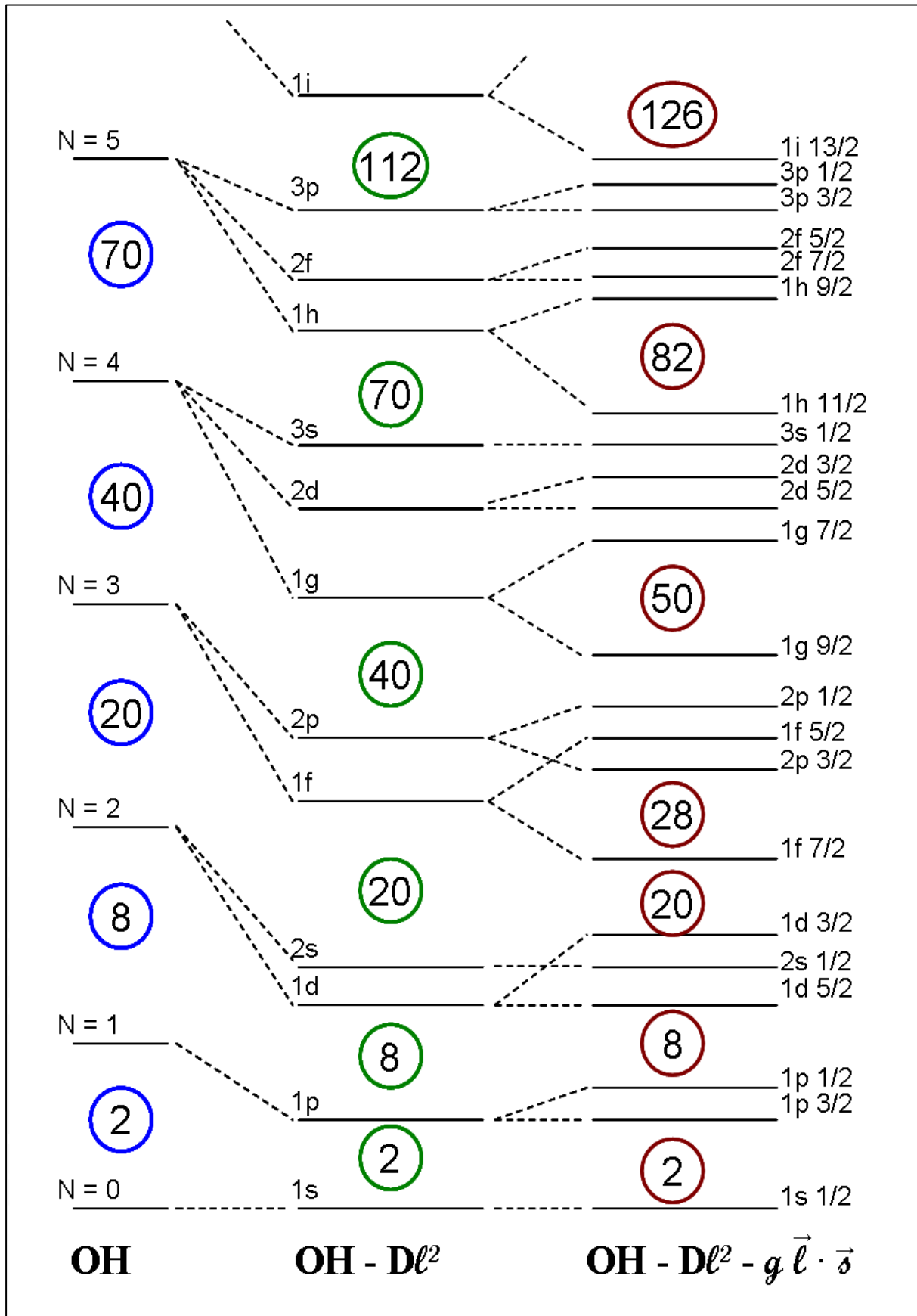


Figure I-7: Diagram of the shell model single-particle orbitals [17].

Despite the success of the *independent particle model* in reproducing all the magic numbers, but it could not be sufficient. For example, the model cannot explain why an even-even nucleus always has a $J^\pi = 0^+$ in the ground state, or more generally, why any even number of similar nucleons couple to a 0^+ state. There is clearly a (residual) interaction between a nucleon “ i ” and a nucleon “ j ”, which favors the coupling of the nucleons with opposing angular momentum.

3.3 The nucleon-nucleon interaction

The *nucleon-nucleon interaction* (N-N) is the interaction between two free nucleons. With a very rare exception, it is assumed in nuclear structure calculations that the degrees of freedom related to the exchange of mesons between nucleons can be replaced by a potential acting between two nucleons [18]. Thus, the determination of the N-N potential appears as one of the fundamental tasks of theoretical nuclear physics. In fact, the binding energy of a nucleus depends critically on the nature of the N-N interaction. Let’s also remember that no experiment has yet succeeded in measuring short-range interaction that connects the nucleons. The determination of the nucleon-nucleon strength is an interesting problem in itself since we have a lot of data by studying the nucleon-nucleon diffusion [18]. We will see later how this effective interaction can be primarily determined in two ways.

4. Beyond the mean field

The independent particle model (mean field) is applicable only for spherical nuclei (closed shell or near to a closed shell). Considering the case of a nucleus with A nucleons (Z protons and N neutrons) interacting to each other, we assume that these nucleons interact in pairs. The spherical mean field provides a global zero-order view of the structure of this nucleus. The correct description of such a nucleus requires taking into account the two-body interaction V_{ij} .

The Hamiltonian of this nucleus is then put in the form [13]:

$$H = \sum_{i=1}^A (T_i + U_i) + \left(\sum_{i>j}^A V_{ij} - \sum_{i=1}^A U_i \right) = H_0 + H_r = \sum_{i=1}^A h_i + H_r \quad (I - 17)$$

H_0 describes the independent movement of nucleons in a 1-body potential U .

h_i denotes the individual Hamiltonian of a nucleon i .

H_r represents the residual two-body interaction, which is considered as a perturbation of the H_0 Hamiltonian by an adequate choice of the mean field U .

The H_r Hamiltonian is generally determined by two methods: the first (used in our calculations) is the shell model with the previously mentioned independent particle model; the second is the Hartree-Fock method.

The Schrodinger's equation of this system is written [13]:

$$H\Psi_\alpha = \left\{ \sum_{i=1}^A (T_i + U_i) + \left(\sum_{i>j}^A V_{ij} - \sum_{i=1}^A U_i \right) \right\} \Psi_\alpha = E\Psi_\alpha \quad (I - 18)$$

where α denotes all quantum numbers.

The eigenwave function Ψ_α is represented by the Slater determinants Φ of H_0 , from which the residual interaction matrix H_r will be diagonalized ($\langle\Phi|H_r|\Phi\rangle$).

Since the size of the matrix increases very quickly with the increasing number of nucleons in the complete Hilbert's space (shown on Fig I-7) so it becomes impossible to proceed to the diagonalization. To overcome this, we choose a subset of configurations guided by physical considerations.

Hilbert's space is divided into three parts [5]:

- ✓ An inert core composed of shells, which are always occupied (usually a magic nucleus with Z_c protons and N_c neutrons).
- ✓ A valence space containing the rest of the active nucleons ($z = Z - Z_c$) and ($n = N - N_c$) which interact via the H_r interaction.
- ✓ An external space formed of orbitals, which are always unoccupied.

The approximation of considering the nucleons occupying the orbits of the core as "inactive" is justified by the existence of a large difference in energy separating these orbits from those immediately superior. For example, the energy difference between the $0p_{1/2}$ and $0d_{5/2}$ subshells is 11.5 MeV [5].

5. Ingredients of the shell model

Any shell model calculation requires the employment of the following three ingredients [5]:

- The definition of a valence space (inert core, active shells).
- The derivation of an effective interaction compatible with the chosen valence space.
- A computational code to build and diagonalize the Hamiltonians.

5.1 Choice of the *valence space*

As previously defined, the inert core (see figureI-8) is often associated with a magic or doubly magic nuclei (${}^4_2\text{He}$, ${}^{16}_8\text{O}$, ${}^{40}_{20}\text{Ca}$, ...) then comes the valence space which could include closed shells but must necessarily contain partial or unfilled shells. If we take our example of ${}^{28}_{14}\text{Si}$, the *normal* positive parity states, are well reproduced within the sd valence space, while the *intruder* negative parity *ones* need a larger valence space such as p-sd-pf space (the probability of excitation of ${}^{28}\text{Si}$ nucleons here are equal), we will explain them well in the next chapter.

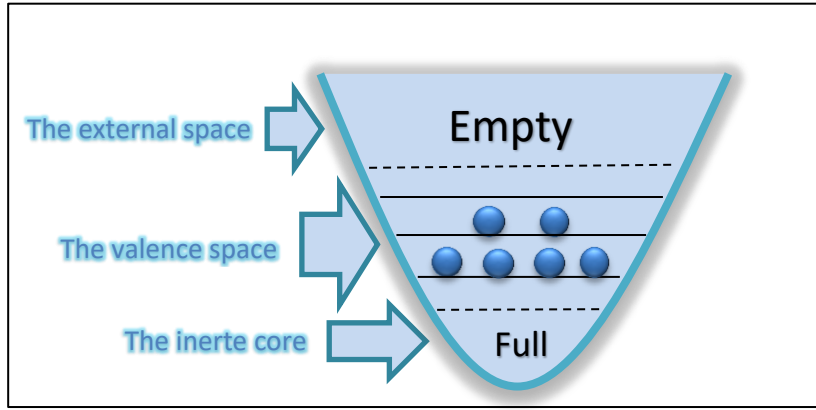


Figure I-8: Diagram of the valence space.

We give some examples of valence (named also model) spaces (truncated from figureI-7):

- ❖ The p shell is a space formed of both orbital $0p_{3/2}$ and $0p_{1/2}$, in which can be described the properties of nuclei with $2 < N, Z < 8$, the inert core is the ${}^4_2\text{He}$.
- ❖ The sd shell valence space is composed of the three orbital $0d_{5/2}$, $1s_{1/2}$ and $0d_{3/2}$, only the positive parity states of nuclei with $8 < N, Z < 20$ can be described, the inert core is the ${}^{16}_8\text{O}$.
- ❖ The pf shell is the space containing the four sub-shells $0f_{7/2}$, $1p_{3/2}$, $0f_{5/2}$ and $1p_{1/2}$ which is adequate for nuclei with $20 < N, Z < 40$, the inert core is the ${}^{40}_{20}\text{Ca}$.

5.2 Effective interaction

Because of the strong short-range repulsion, the nucleon-nucleon interaction cannot be used directly in shell model calculations [19]. Therefore, these calculations are based on the definition of an effective interaction that is strongly connected to the valence space used.

There are two types of effective interactions [19]:

- Realistic effective interaction.
- Phenomenological effective interaction.

The first type is realistic calculated directly from nucleon-nucleon potential. The second type is phenomenology, which consists in selecting the initiating Hamiltonians and in considering the individual energies and the cross-matrix elements as parameters to be adjusted directly on the experimental data, as it was done for the development of the PSDPF interaction [5] used in the calculation of our work.

5.3 The computational code

The two shell model codes developed in Strasbourg are the ANTOINE code [20, 21] and the code NATHAN [21, 22]. We will use the code NATHAN in our calculations.

For our knowledge, we mention some of the other international codes: GLASGOW [23], VECSSSE [24], MSHELL [25], REDSTICK [26], RITSSCHIL [27], OXBASH [28], and DUPSM [29].

In this chapter, we have presented the basic concepts of the shell model, which makes it possible to describe the nuclear structure.

In the next chapter we will introduce the sd shell nuclei, a region of our current work, and their properties as well the PSDPF interaction.

Chapter II

The sd-Shell Nuclei

Nuclei in the sd shell (i.e. with valence nucleons confined in the orbitals $d_{5/2}, s_{1/2}$ and $d_{3/2}$) have a number of neutrons N and protons Z between magic numbers 8 and 20. Thus, this area is limited by the two doubly magic nuclei ^{16}O and ^{40}Ca (see Fig I-7). These nuclei have been studied since 1960 and their structure has been the subject of many experimental and theoretical investigations. The chart regrouping these nuclei is presented in Fig II-1.

In this chapter we will introduce some properties of the sd-shell nuclei, and we present the PSDPF interaction developed by M. BOUHELAL [5,6] to reproduce the spectroscopic properties and the structure of these nuclei.

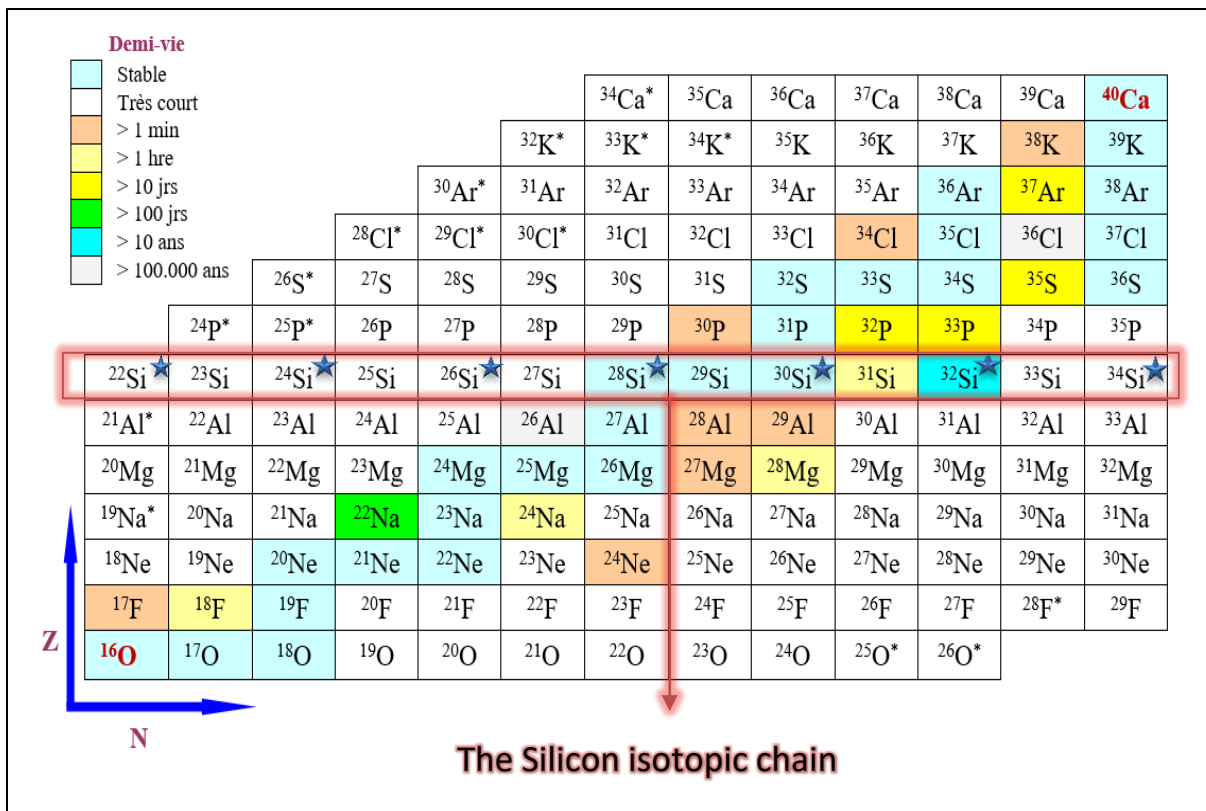


Figure II-1: Chart of sd shell nuclei [10]. For nuclei selected with star «*» the ground state is unbound, i.e. unstable compared to particle emission. Nuclei with «★» are all even-A silicon isotopes.

The sd shell area includes 146 experimentally known nuclei, 26 of them are stable. These sd-shell nuclei are characterized, at low excitation energies, by the coexistence of spherical normal positive parity (+) and intruder negative parity (–) states (also intruder collective positive parity may also be found) [10].

Nuclei of particular interest in our work are the even-A Si isotopic chain. The Si isotopes ($Z=14$) are located in the middle of the sd shell.

1. The spherical normal states

The normal positive parity states correspond to the movement of A-16 nucleons within the sd shell, since the 16 nucleons of the core are considered to be inert. The valence space in this case is limited to the sd orbitals, $1d_{5/2}$, $2s_{1/2}$, $1d_{3/2}$, and thus the inert core is ^{16}O , i.e. the s and p shells are filled and inactive.

In the sd shell nuclei, these states appear at low excitation energies for the mass range varies from $A=17$ to $A=39$. This implies the 0 particles and 0 holes configuration (0p–0h), hence the name of the normal states is also $0\hbar\omega$.

Various interactions have been developed to describe the spherical normal states, in particular the USD [30, 31] (Universal SD interaction) or the updated interactions USDA/B [32].

2. The intruder states

Not all states of the nuclei in the sd shell can be reproduced by the above interactions (by increasing the excitation energy and/or moving away from the stability valley, intruder states appear) [5]. In an sd shell nucleus, two types of intruder states can exist with positive- or negative- parity. These states differ in their parities but result from the promotion of nucleons between major shells; from p to sd or sd to pf shells. Thus, intruder states have configurations outside the sd valence space.

2.1 The intruder spherical negative parity states

In these same nuclei, there is also a set of negative parity states of type (1p–1h) named also $1\hbar\omega$ states, reported among the adopted levels [10]. Such states result from the promotion of one nucleon from shells p to sd (for nuclei at the beginning of the sd shell around ^{16}O) or from sd to pf (for nuclei at the end of the sd shell near ^{40}Ca). Their SM description requires in addition of the sd shell, the inclusion of the p and the pf shells needed to treat the p–sd and sd–pf excitations which are mainly responsible for the negative parity states at the beginning and at the end of the sd shell, respectively [5,6]. Concerning nuclei at the middle of sd shell, it is found that the $1\hbar\omega$ states may have a competition between the two excitations p–sd and sd–pf. Diverse interactions have been developed to describe separately these states in these two regions. The interaction that describes in a consistent way these states

in all nuclei throughout the sd shell is the PSDPF developed by M. BOUHELAL [5, 6]. The sd-shell nuclei having known negative parity intruder states are shown in Fig II-2.

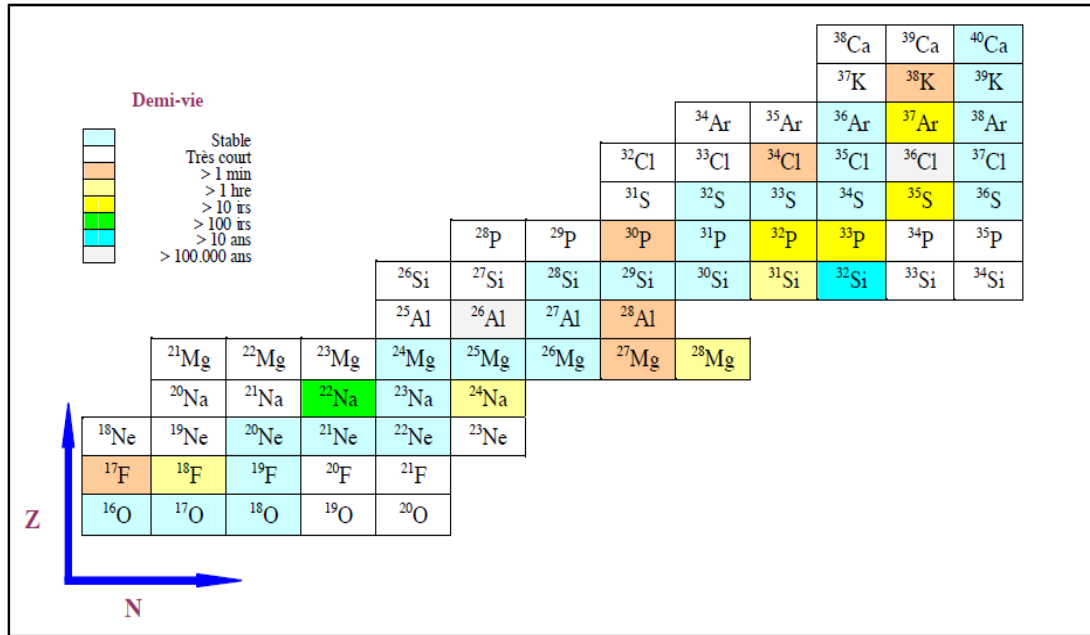


Figure II-2: Chart of sd nuclei with known negative parity intruder states [10].

2.2 The positive- and negative- parity intruder states

In the sd nuclei, intruder states with positive- and/ or negative- parity, whose configurations is outside the sd valence space, can coexist. These states result from the promotion of one nucleon or more across major shells, and are thus of type (np–nh) called also $n\hbar\omega$ states, $n>1$. The states in question here have positive parity if the jump numbers between the two major shells (p–sd or sd–pf) are even (even n). Recent shell model calculations have shown that this type of levels result mostly from 2p-2h excitations ($2\hbar\omega$) or 4p-4h excitations ($4\hbar\omega$). This means that these nuclei are generally deformed and these states contribute strongly to the collective character of the nucleus, as it is observed near the doubly magic nuclei ^{16}O and ^{40}Ca . States corresponding to odd excitation number, odd n, have negative parity, example the $3\hbar\omega$ states of configuration (3p-3h) type.

3. The PSDPF interaction

In order to describe simultaneously both negative and positive parity states in sd shell nuclei, and the transitions between these different states, we use the PSDPF interaction developed in Strasbourg by M. Bouhelal et al. [5,6]. In this case, the core used is restricted to the ^4He doubly magic nucleus and the valence space includes the p, sd and pf shells (containing 9 sub-shells).

3.1 The construction of the PSDPF interaction

- ❖ The aim: description of 0 and $1\hbar\omega$ states in sd shell nuclei.
- ❖ The model space used: ^4He core, the 9 p-sd-pf sub-shells.
- ❖ One nucleon jump between major shells is allowed.

3.2 Shell model ingredients in case of sd shell nuclei

- ✓ Valence space: the full p-sd-pf model space.
- ✓ The compatible interaction with this space: the PSDPF interaction.
- ✓ Code of calculation: the shell model code NATHAN [20, 21].

The Si isotopic chain, in which we are particularly interested in this work, is located in the middle of the sd shell. Accordingly, the $1\hbar\omega$ states in these isotopes have a competition between the two excitations p-sd and sd-pf. Both positive and negative parity states in these isotopes can simultaneously be described within the full p-sd-pf valence space with ^4He core and using the PSDPF interaction, as we will see in the next chapter.

4. Application of the shell model

Some of the shell model applications are the calculation of the parity, spin and isospin corresponding to the energy level in the nucleus. We give in the next sections a brief definition of each of these observables.

4.1 Parity

It is possible to show that the stationary states in nucleus, solutions of the time independent Schrodinger equation, have a definite parity that depends of the sum of l values of all the individual nucleons. Actually, the more technically correct statement is that $\Pi = (-1)^{\sum l}$. Two possible values are obtained for the parity, $\Pi = 1$ (even parity), and $\Pi = -1$ (odd parity) [13].

4.2 Nuclear spin

Nuclear spin is a physical quantity characteristic of a nucleus that describes its magnetic properties. The nuclear spin can be described by a vector operator J of module $\|J\|$ whose projection on a fixed axis is denoted J_z . The choice of the vertical direction OZ as the quantization axis is convenient but is not imperative. It is dictated by the fact that this axis is chosen as the direction of the static magnetic field in the following. The quantum description

involves operators, which is expressed as a function of the quantum number of nuclear spin J , by the following relation:

$$\|J\| = \frac{h}{2\pi} \sqrt{j(j+1)} \quad (II-1)$$

(h is the Planck constant $h = 6.62 \cdot 10^{-34} \text{J}\cdot\text{s}$).

Particular cases for spin & parity of the nuclei's ground state:

Even-Even Nuclei: $J^\Pi = 0^+$.

Even-Odd Nuclei: J^Π given by unpaired nucleon or hole; $\Pi = (-1)^l$.

Odd-Odd Nuclei: J^Π is obtained using the J values of the unpaired p and n , then apply j - j coupling.

$$\text{i.e. } |J_p - J_n| \leq J \leq J_p + J_n \quad ; \quad \Pi = (-1)^{l_p+l_n}$$

An example is shown on Fig II-3.

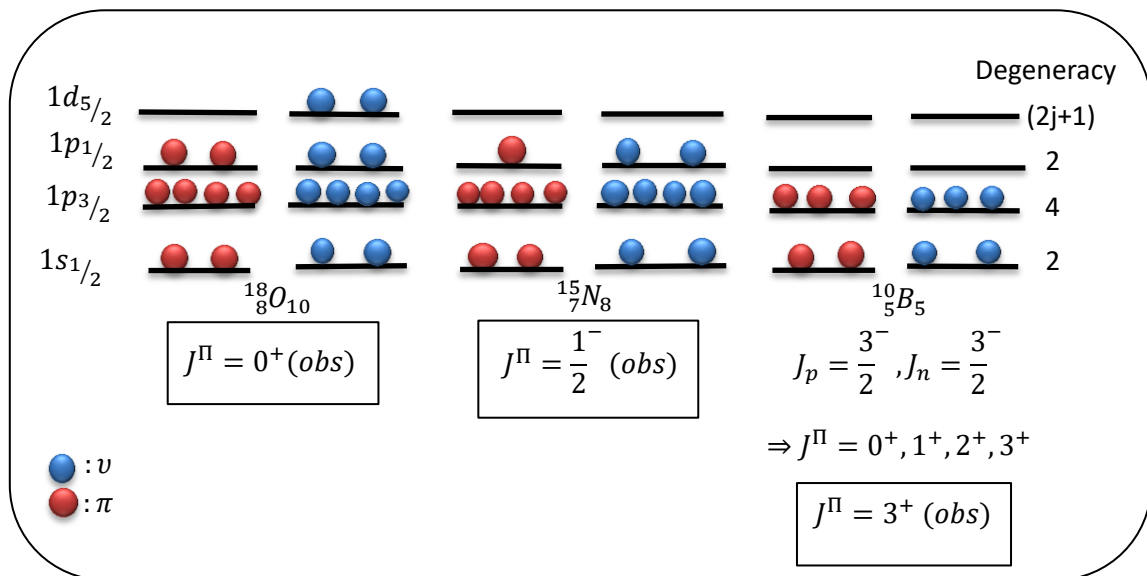
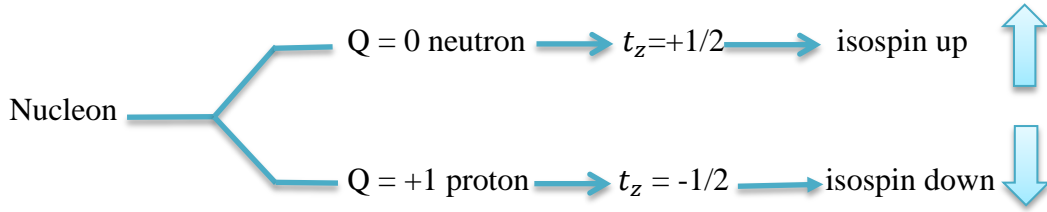


Figure II-3: Different nucleon distributions that gives the ground state J^Π values in some nuclei. Obs: Observed state

4.3 Isospin

After the discovery of the neutron by Chadwick [3], W. Heisenberg proposed the isospin in 1932 [33] in the aim of constructing a mathematical basis that represents the similarity of proton-neutron with respect to the strong nuclear force. Indeed, the masses of the proton and the neutron are very close, $m_p = 938.272013(23) \text{ MeV}/c^2$ and $m_n = 939.565346(23) \text{ MeV}/c^2$ [34], and the mass ratio is about one, i.e., $\frac{m_n}{m_p} = 1.001378$.

Assuming that the proton and the neutron have very similar masses, Heisenberg proposed to consider them as two different states of charge of the same nucleon. To distinguish between them he introduced a new observable, the isospin t whose projection on the OZ axis is t_z , and assigning $t_z = +1/2$ for the neutron and $t_z = -1/2$ for the proton [13].



The mathematical formalism of the isospin used by Heisenberg is analogous to the formalism of the intrinsic spin developed by Pauli.

The single-particle wave functions of a neutron and a proton can be expressed with the help of $t = 1/2$ spinors as [13]:

$$\varphi_n(r) = \varphi(r) \begin{pmatrix} 1 \\ 0 \end{pmatrix} \quad \text{et} \quad \varphi_p(r) = \varphi(r) \begin{pmatrix} 0 \\ 1 \end{pmatrix} \quad (\text{II} - 2)$$

Similarly, to the angular momentum, we can introduce an isospin operator, a vector $t = \frac{1}{2}\tau$, where three components of the vector τ have a form of the Pauli matrices:

$$\tau_x = \begin{pmatrix} 0 & 1 \\ 1 & 0 \end{pmatrix}, \tau_y = \begin{pmatrix} 0 & -i \\ i & 0 \end{pmatrix}, \tau_z = \begin{pmatrix} 1 & 0 \\ 0 & -1 \end{pmatrix} \quad (\text{II} - 3)$$

On the other hand, we can summarize:

$$Q = \sum_i^z q_p = Ze \Rightarrow Z = \frac{Q}{e} \Rightarrow T_z = \frac{N}{2} - \frac{Q}{2e} = \frac{A}{2} - \frac{Q}{e} \Rightarrow Q = \left(\frac{A}{2} - T_z\right)e \quad (\text{II} - 4)$$

Where Q is the electric charge of a nucleus, and T_z is the projection of the total isospin, A denoting the total number of nucleons in nucleus

4.4 Shell occupation

The Eigenfunctions are obtained as a product of a single-particle wave function [13].

$$\Psi_{a_1 a_2 \dots a_A}(1, 2, \dots, A) = \prod_{A=1}^k \Phi_{a_k}(r(k)) \quad (\text{II} - 5)$$

For identical nucleons, i.e. either neutrons or protons, the simple product wave function given by eq. (II-5) is not appropriate, since it must describe indistinguishable particles.

For nucleons, which are fermions. This implies according to the Pauli exclusion principle that the wave functions should be anti-symmetric. For two particles, the normalized, anti-symmetric wave function is written as [13]:

$$\Psi_{ab}(1,2) = \sqrt{\frac{1}{2}} [\Phi_a(1)\Phi_b(2) - \Phi_a(2)\Phi_b(1)] \quad (\text{II} - 6)$$

Or, equivalently, as a Slater determinant

$$\Psi_{ab}(1,2) = \sqrt{\frac{1}{2}} \begin{vmatrix} \Phi_a(1) & \Phi_a(2) \\ \Phi_b(1) & \Phi_b(2) \end{vmatrix} \quad (\text{II} - 7)$$

The wave function $\Psi_{ab}(1,2)$ is antisymmetric, since the operator P_{12} that interchanges particles 1 and 2 yields to $P_{12}\Psi_{ab}(1,2) = \Psi_{ab}(2,1) = -\Psi_{ab}(1,2)$. The normalization of $\Psi_{ab}(1,2)$ is guaranteed by the orthonormality of the single-particle wave functions Φ_a and Φ_b .

Similarly, a normalized, antisymmetric A-particle wave function is defined by the Slater determinant:

$$\Psi_{a_1 a_2 \dots a_A}(1,2, \dots, A) = \frac{1}{\sqrt{A!}} \begin{vmatrix} \Phi_{a_1}(1) & \Phi_{a_1}(2) & \Phi_{a_1}(A) \\ \Phi_{a_2}(1) & \Phi_{a_2}(2) & \Phi_{a_2}(A) \\ \vdots & \vdots & \vdots \\ \Phi_{a_A}(1) & \dots & \Phi_{a_A}(A) \end{vmatrix} \quad (\text{II} - 8)$$

Explicit use of these determinantal wave functions soon leads to complicated expressions for matrix elements [13].

The quantum wave is not located anywhere in the space like a real wave and it possesses no energy. Since the quantum wave does not carry energy it is not directly detectable. The presence of the quantum wave is identified after many particle events. According to this interpretation, the quantum wave described usually with the quantum function $\psi(\vec{r}, t)$. The probability of finding the particle (nucleon) in point r and at time t in the volume element $d^3\vec{r}$ (inside the nucleus volume) is defined as [35]:

$$dp = |\Phi(\vec{r}, t)|^2 dv < 1 \rightarrow \text{probability of finding the particle (nucleon)} \quad (\text{II} - 9)$$

$\Phi(\vec{r}, t)$ is the particle wavefunction; $\vec{r} = x\vec{i} + y\vec{j} + z\vec{k}$; $dv = dx dy dz = d^3\vec{r}$

As Fig II-4 indicated, the particle (nucleon) could be found anywhere in space (nucleus), however it is most likely to be found where the probability of its wave function is large. By integrating the Eq. (II-9) over all the possible positions in the space inside the nucleus, the integral will give the total probability of finding the nucleon in all the nucleus volume. Since the nucleon will certainly be found somewhere inside the nucleus, the integral must be equal to unity.

$$p = \iiint_v |\phi(\vec{r}, t)|^2 dv = 1 \quad (II - 10)$$

v is the volume occupied by a nucleon.

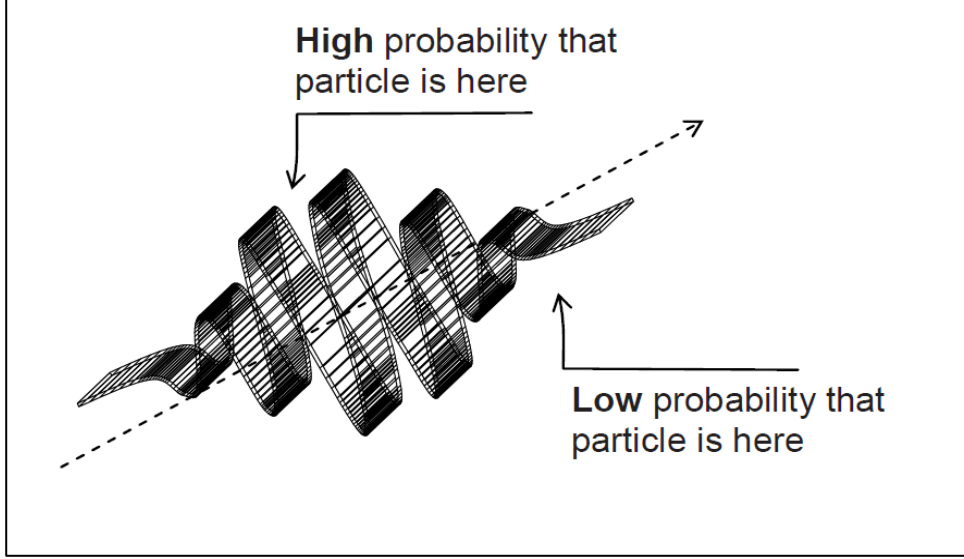


Figure II-4: Wave-particle duality [35].

For a nucleon moving along one dimension, the Eq. (II-10) takes the following form:

$$p = \int_{-\infty}^{+\infty} |\Phi(x, t)|^2 dx = 1 \quad (II - 11)$$

The probability of finding a J^Π state (a certain slater determinant) that results from a certain distribution of nucleons forming the nucleus ${}^A_Z X_N$ is given by:

$$dP = |\Psi(\vec{r}, t)|^2 dV < 1 \quad (II - 12)$$

V is the nucleus' volume.

The probability of finding a J^Π state resulting from all the different distribution of the nucleons inside the nucleus (all slater determinants) is given by:

$$P = \iiint_V |\Psi(\vec{r}, t)|^2 dV = 1 \quad (II - 13)$$

5. Nucleons Distribution

We have seen that a nucleus ${}^A_Z X_N$, where Z and N are magic numbers, acts as an inert core. The total angular momentum of this core is zero and a nucleon moving outside of it, feels the interaction of the nucleons inside the core as a whole. The core induces a central field which generates the shell model set of single-particle states, that is the individual orbits represented

on Fig I-7. Each one of the nucleons in the nucleus occupies one of those orbits in the sequence shown on Fig I-7.

For instance, the + states in sd nuclei result from the distribution of the valence nucleons within the sd shell formed of the 3 orbits $1d_{5/2}$, $2s_{1/2}$ and $1d_{3/2}$, and considering $^{16}_8\text{O}_8$ nucleus as a core. As an example, we consider the $^{26}_{14}\text{Si}$ nucleus having 10 valence nucleons outside ^{16}O , whose 8 neutrons and 8 protons occupying the orbits $1s_{1/2}$, $1p_{3/2}$ and $1p_{1/2}$. We illustrate on Figure II-5, the distribution of protons and neutrons to form the ^{26}Si ground state.

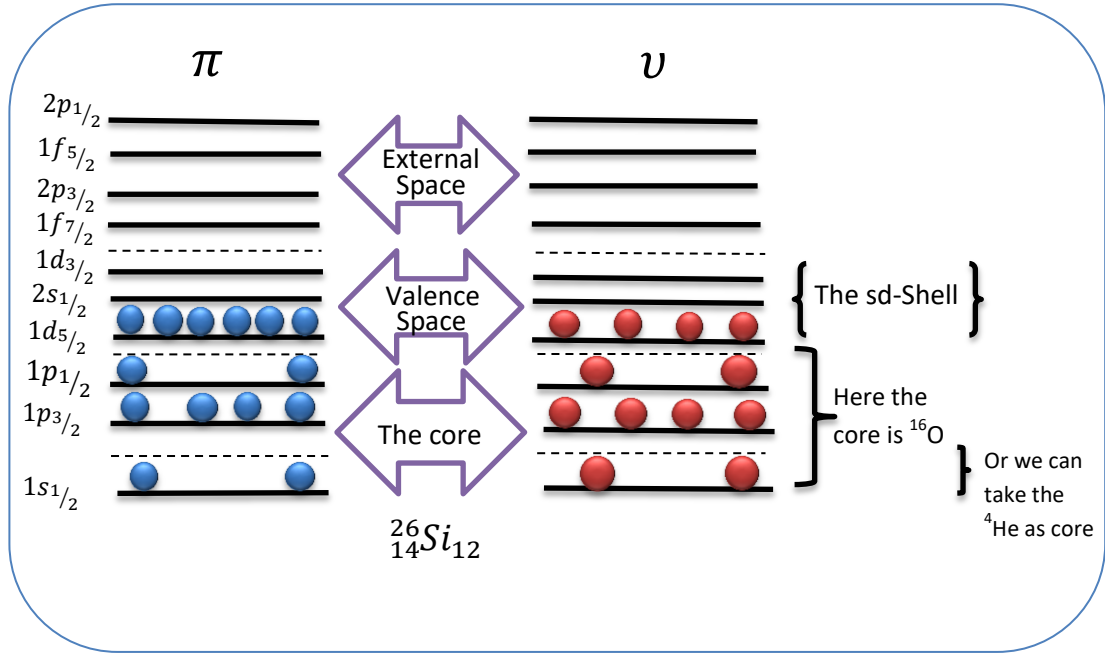


Figure II-5: Distribution of nucleons forming the ground state of ^{26}Si .

- Using the PSDPF interaction and the NATHAN code, we calculated the probability to distribute nucleons called also *shell occupation probabilities* to obtain the first + and – states excited in ^{26}Si , which are 2^+ and 3^- respectively. The nucleon distribution that has the highest probability for each of these states is illustrated on Fig II-6.

From Fig II-6 we remark that:

- ✚ The PSDPF interaction predicts that first excited state of parity 2^+ has the same configuration (distribution of nucleons) as that of the ground state corresponding to the filling of the orbit $1d_{5/2}$, but with only 18.6% probability.
- ✚ The first – excited state resulting from one neutron jump from the $1p_{1/2}$ shell to the $1d_{5/2}$ with only a probability of only 8%.

The small values of the highest probabilities mean that these states have fragmented configurations resulting from different nucleon distribution within the sd shell for the + state and p–sd for the – state.

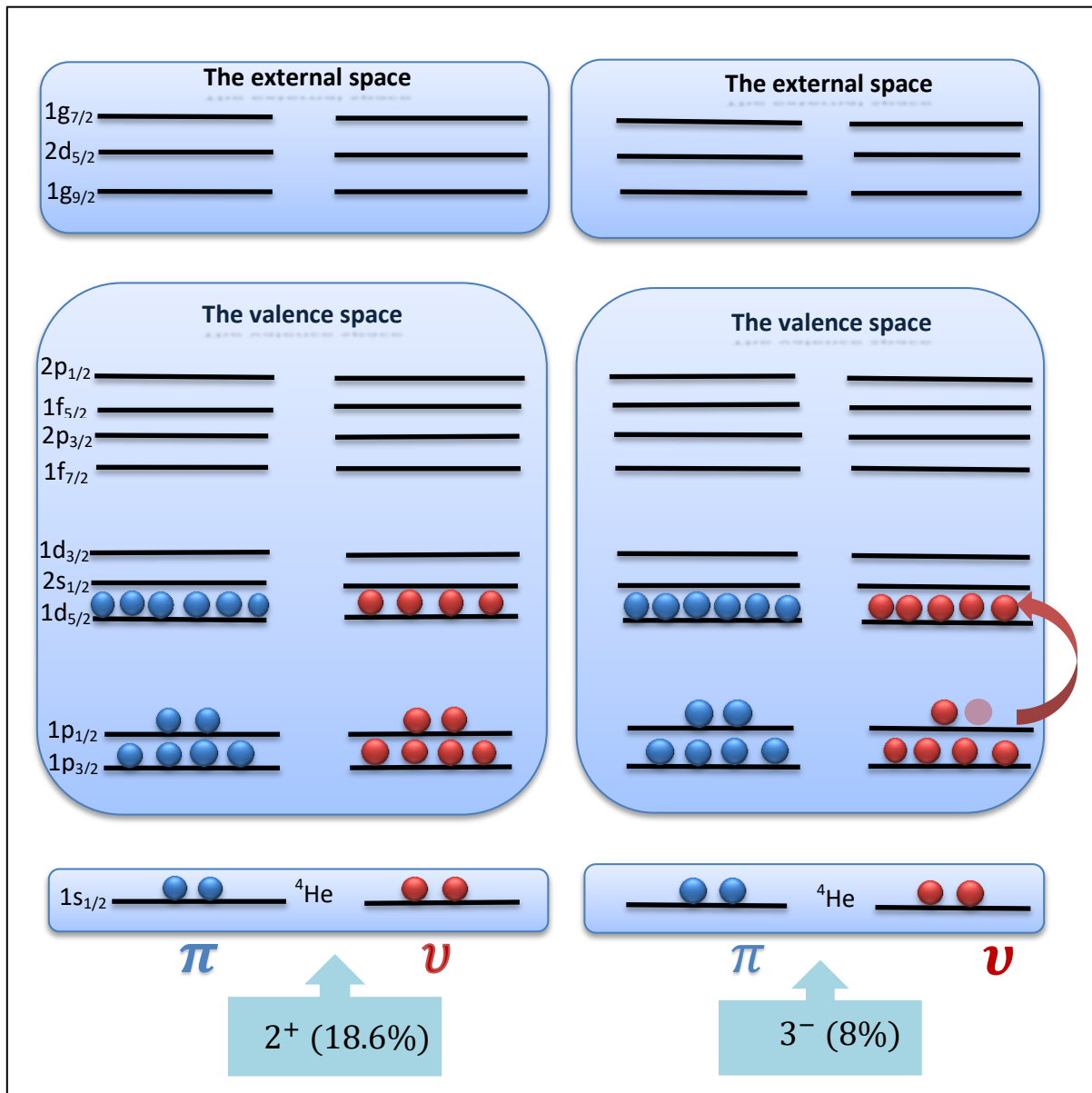


Figure II-6: Schematic of the configurations of the first excited states 2^+ and 3^- in the $^{26}_{14}\text{Si}$.

All the calculated probabilities of nucleons distributions for 2^+ and 3^- states in ^{26}Si are presented on Table II-1 and Table II-2, respectively.

◆ For the state 2⁺

Probability	The distribution for neutrons									The distribution for protons								
	1p	1p	1d	2s	1d	1f	2p	1f	2p	1p	1p	1d	2s	1d	1f	2p	1f	2p
	1/2	3/2	5/2	1/2	3/2	7/2	3/2	5/2	1/2	1/2	3/2	5/2	1/2	3/2	7/2	3/2	5/2	1/2
0.0100 6394	2	4	2	0	2	0	0	0	0	2	4	5	1	0	0	0	0	0
0.0122 2118	2	4	2	0	2	0	0	0	0	2	4	6	0	0	0	0	0	0
0.0110 7218	2	4	2	1	1	0	0	0	0	2	4	4	1	1	0	0	0	0
0.0119 1692	2	4	2	1	1	0	0	0	0	2	4	4	2	0	0	0	0	0
0.0112 9481	2	4	2	1	1	0	0	0	0	2	4	5	0	1	0	0	0	0
0.0137 6571	2	4	2	1	1	0	0	0	0	2	4	5	1	0	0	0	0	0
0.0200 0966	2	4	2	1	1	0	0	0	0	2	4	6	0	0	0	0	0	0
0.0131 8006	2	4	2	2	0	0	0	0	0	2	4	5	1	0	0	0	0	0
0.0110 3425	2	4	3	0	1	0	0	0	0	2	4	4	0	2	0	0	0	0
0.0171 5336	2	4	3	0	1	0	0	0	0	2	4	4	1	1	0	0	0	0
0.0107 5249	2	4	3	0	1	0	0	0	0	2	4	4	2	0	0	0	0	0
0.0289 4563	2	4	3	0	1	0	0	0	0	2	4	5	0	1	0	0	0	0
0.0200 7730	2	4	3	0	1	0	0	0	0	2	4	5	1	0	0	0	0	0
0.0201 2629	2	4	3	0	1	0	0	0	0	2	4	6	0	0	0	0	0	0
0.0180 7002	2	4	3	1	0	0	0	0	0	2	4	4	0	2	0	0	0	0
0.0212 4819	2	4	3	1	0	0	0	0	0	2	4	4	1	1	0	0	0	0
0.0329 9206	2	4	3	1	0	0	0	0	0	2	4	4	2	0	0	0	0	0
0.0149 0352	2	4	3	1	0	0	0	0	0	2	4	5	0	1	0	0	0	0
0.0263 1051	2	4	3	1	0	0	0	0	0	2	4	5	1	0	0	0	0	0

0.0614 3499	2	4	3	1	0	0	0	0	0	2	4	6	0	0	0	0	0	0
0.0100 6922	2	4	4	0	0	0	0	0	0	2	4	2	2	2	0	0	0	0
0.0139 0381	2	4	4	0	0	0	0	0	0	2	4	3	1	2	0	0	0	0
0.0134 6783	2	4	4	0	0	0	0	0	0	2	4	3	2	1	0	0	0	0
0.0426 5504	2	4	4	0	0	0	0	0	0	2	4	4	0	2	0	0	0	0
0.0322 9502	2	4	4	0	0	0	0	0	0	2	4	4	1	1	0	0	0	0
0.0508 4477	2	4	4	0	0	0	0	0	0	2	4	4	2	0	0	0	0	0
0.0279 9412	2	4	4	0	0	0	0	0	0	2	4	5	0	1	0	0	0	0
0.0673 0012	2	4	4	0	0	0	0	0	0	2	4	5	1	0	0	0	0	0
0.1857 5723	2	4	4	0	0	0	0	0	0	2	4	6	0	0	0	0	0	0

Table II-1: Calculations of the probability for the different configurations (*shell occupation probabilities*) giving rise the first excited state 2^+ .

◆ For the state 3

Proba bility	The distribution for neutrons									The distribution for protons								
	1p	1p	1d	2s	1d	1f	2p	1f	2p	1p	1p	1d	2s	1d	1f	2p	1f	2p
	1/2	3/2	5/2	1/2	3/2	7/2	3/2	5/2	1/2	1/2	3/2	5/2	1/2	3/2	7/2	3/2	5/2	1/2
0.0115 8688	2	4	4	0	0	0	0	0	0	2	3	6	0	1	0	0	0	0
0.0110 0057	2	4	4	0	0	0	0	0	0	2	4	5	0	0	1	0	0	0
0.0133 3954	1	4	3	1	1	0	0	0	0	2	4	4	1	1	0	0	0	0
0.0150 4239	1	4	3	2	0	0	0	0	0	2	4	4	2	0	0	0	0	0
0.0148 5489	1	4	4	0	1	0	0	0	0	2	4	5	0	1	0	0	0	0
0.0117 5618	1	4	4	1	0	0	0	0	0	2	4	3	2	1	0	0	0	0

0.0165 4240	1	4	4	1	0	0	0	0	0	2	4	4	1	1	0	0	0	0
0.0112 1993	1	4	4	1	0	0	0	0	0	2	4	4	2	0	0	0	0	0
0.0318 3491	1	4	4	1	0	0	0	0	0	2	4	5	1	0	0	0	0	0
0.0100 9188	1	4	5	0	0	0	0	0	0	2	4	2	2	2	0	0	0	0
0.0104 5243	1	4	5	0	0	0	0	0	0	2	4	3	2	1	0	0	0	0
0.0209 9455	1	4	5	0	0	0	0	0	0	2	4	4	0	2	0	0	0	0
0.0137 9332	1	4	5	0	0	0	0	0	0	2	4	4	1	1	0	0	0	0
0.0381 5501	1	4	5	0	0	0	0	0	0	2	4	4	2	0	0	0	0	0
0.0802 3798	1	4	5	0	0	0	0	0	0	2	4	6	0	0	0	0	0	0
0.0114 1575	2	3	4	0	1	0	0	0	0	2	4	4	2	0	0	0	0	0
0.0232 3191	0	0	0	0	0	0	0	0	0	0	0	0	0	0	0	0	0	0

Table II-2: Calculations of the probability for the different configurations (*shell occupation probabilities*) giving rise the first excited state 3⁻.

In this chapter, after defining the sd shell area of nuclei; we presented some of the sd shell nuclei properties and we introduced the interaction that developed to describe both the normal positive parity and intruder negative parity states.

Chapter III

Systematic study of the even-A Silicon isotopic chain

One of the main aims of researches in nuclear physics is to describe the ground and excited states of all nuclei in the periodic table. In the present work, we used the PSDPF interaction to calculate the energy spectra of positive and negative parity states of the sd-shell even-A silicon isotopes. A systematic study of the four + and – states will be presented in this chapter.

- As a preface to our work in this chapter and before our systematic study for the even-A silicon isotopic chain, we give some information about the silicon element.

1. Properties of the Silicon element

1.1 Interesting facts

- Discoverer: Jöns Jacob Berzelius.
- Discovery date 1823.
- Discovered in: Sweden.
- Appearance: dark grey with a bluish ting.
- Classification: Semi-metallic.
- Origin of name: from the Latin word "silicis" meaning "flint".
- Uses: computer, chips, lubricant, nuclear radiation detectors, semi-conductor integrated circuits, solar energy.
- Obtained from: clay, granite, quartz, and sands.
- The second most abundant element in our planet is Silicon.
- Silicon is made in stars with a mass of eight or more earth sun.
- The lowest acceptable purity for electronic grade silicon is 99.9999999%.



1.2 The physical properties

- Name: Silicon.
- Symbol: Si.
- Atomic number: 14.
- Standard solid state: at 298K.
- Classification: semi-metallic.
- Group in periodic table: 14.
- Period in periodic table: 3.
- Block in periodic table: p.

- Shell structure: 2.4.8
- Electron Configuration: $[Ne]3S^23P^1$.

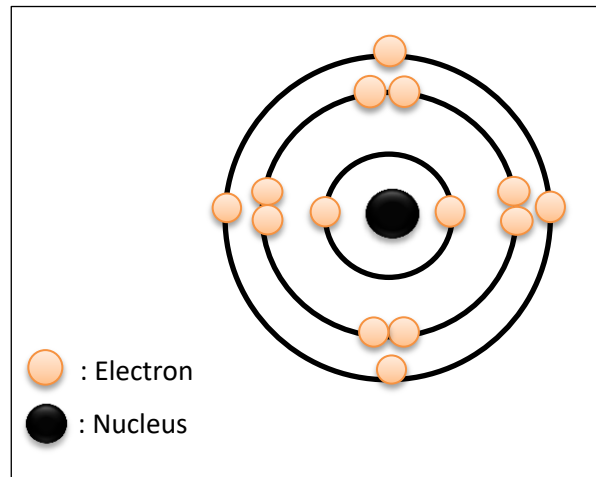


Figure III-1: The atomic model of the silicon atom.

The observation of 23 silicon isotopes has been reported so far, including 3 stable, 6 proton-rich, and 14 neutron-rich isotopes. The sd shell region of our interest contains only 13 silicon isotopes from $A=22$ to $A=35$.

2. Properties of Silicon isotopes

There are four natural isotopes of silicon (Si) existing in the environment: ^{28}Si , ^{29}Si , ^{30}Si and ^{32}Si . The first three isotopes are stable and the last one is radiogenic. The relative abundance of ^{28}Si , ^{29}Si and ^{30}Si is 92.23%, 4.67% and 3.10%, respectively [36]. In the 1920s, all three stable silicon isotopes had been discovered. Mass spectrometric studies on Silicon isotope variation in the natural environment started in the 1950s. In the 1970s, extensive studies on silicon isotope compositions of meteorites and rocks were made [36].

In addition to the previously mentioned natural isotopes, there are 9 other artificial isotopes belonging to the sd shell region, ^{22}Si , ^{23}Si , ^{24}Si , ^{25}Si , ^{26}Si , ^{27}Si , ^{31}Si , ^{33}Si , ^{34}Si .

We focus, particularly in our study, just on the even- A silicon isotopes.

2.1 The even- A silicon isotopes

We present here the properties of the even- A silicon isotopes taken from international nuclear bank [10].

- ❖ ²²Si: Saint-Laurent et al. discovered ²²Si in 1987 in the paper "Observation of a bound $T_Z = -3$ nucleus: ²²Si" [37].
 - ✓ $Z=14; N=8; J^\Pi = 0^+$.
 - ✓ Half-life 29 ms. Mass = (22.03579 ± 5.40) AMU.
 - ✓ Binding energy/A = (6058 ± 2.3) keV.

- ❖ ²⁴Si: In the 1979 paper "Decay of a new isotope, ²⁴Si: A test of the isobaric multiplet mass equation" Äystö et al. Described the first observation of ²⁴Si [38].
 - ✓ $Z=14; N=10; J^\Pi = 0^+$.
 - ✓ Half-life 140 ms. Mass = (24.011353 ± 2.1) AMU.
 - ✓ Binding energy/A = (7167.2 ± 0.8) keV.

- ❖ ²⁶Si: was identified in 1960 by Robinson and Johnson in "Decay of ²⁶Si" [39].
 - ✓ $Z=14; N=12; J^\Pi = 0^+$.
 - ✓ Half-life (2.1 ± 0.3) s, this half-life agrees with the presently accepted value of (2.234 ± 1.3) s. Mass = (25.9923338 ± 1.1) AMU.
 - ✓ Binding energy/A = (7924.708 ± 0.4) keV.

- ❖ ²⁸Si: Aston discovered ²⁸Si in 1920 as reported in "The constitution of the elements" [40].
 - ✓ $Z=14; N=14; J^\Pi = 0^+$.
 - ✓ Half-life: Stable. Mass = (27.976926535 ± 0.5) AMU.
 - ✓ Binding energy/A = 8447.744 keV. Abundance = 92.223%.

- ❖ ³⁰Si: In the 1924 paper "Isotope effects in the band spectra of boron monoxide and Silicon nitride" Mulliken reported the observation of ³⁰Si [41].
 - ✓ $Z=14; N=16; J^\Pi = 0^+$.
 - ✓ Half-life: Stable. Mass = (29.973770136 ± 2.3) AMU.
 - ✓ Binding energy/A = (8520.654 ± 0.1) keV. Abundance = 3.092%.

- ❖ ³²Si: Lindner identified ³²Si in the 1953 paper "New nuclides produced in chlorine spallation" [42].
 - ✓ $Z=14; N=18; J^\Pi = 0^+$.
 - ✓ Half-life: it was found to have a maximum probable half-life of 710 years. Mass = (31.9741515 ± 0.3) AMU.
 - ✓ Binding energy/A = (8481.468 ± 0.9) keV. Abundance = None.

- ❖ ³⁴Si: Artukh et al., discovered ³⁴Si, in the 1971 paper "New isotopes ^{29,30}Mg, ^{31,32,33}Al, ^{33,34,35,36}Si, ^{35,36,37,38}P, ^{39,40}S, and ^{41,42}Cl produced in bombardment of a ²³²Th target with 290 MeV ⁴⁰Ar ions" [43].

- ✓ $Z=14; N=20; J^\pi = 0^+$.
- ✓ Half-life: 2.77 s 20. Mass= (33.978575 ± 1.5) AMU.
- ✓ Binding energy/A= (8336.1 ± 0.4) keV.

2.2 Experimental review of excitation energies in even-A Silicone Isotopes

Investigation of nuclear properties and the laws governing the structure of nuclei is an active and productive area of physical research. Here, we collected the experimental excitation energies; spins and parities J^π of the even-A silicon isotopes' states up to the fourth – state from ^{22}Si to ^{34}Si . Since nuclei with $N < Z$ are less studied due to Coulomb repulsion between protons, we compare them to their mirrors. We present and discuss these properties case by case. We remind that nuclei having an even-A number of nucleons have a $J^\pi = 0^+$ ground state.

The ^{22}Si case

^{22}Si		^{22}O	
E level THEO (MeV)	J^π	E level (MeV)	J^π
0.0	0^+	0.0	0^+
1.75	2^{+*}	3.199	2^+
2.5	0^{+*}	4.584	(3^+)
4.75	4^{+*}	4.909	(0^+)
		5.800	
		6.512	(2^+)
		6.938	(4^+)
		7.649	$(0^-, 1^-, 2^-)$
		8.783	$(0^-, 1^-, 2^-)$
		20.554	$(0^-, 1^-, 2^-)$
		13.298	$(0^-, 1^-, 2^-)$

Table III-1: Comparison of the first excited states in the mirror nuclei ^{22}Si and ^{22}O [10],
* States taken from Ref [44].



to make it clear here are the reasons of comparing just the isotopes ^{22}Si , ^{24}Si , ^{26}Si with their mirror nuclei ^{22}O , ^{24}Ne , and ^{26}Mg .

- ✓ Mirror nuclei have same structure and same excitation energy, the energy differences is due to Coulomb interaction.
- ✓ To answer the question, when is the difference in Coulomb energy occur in these mirrors, the number of neutrons is less than the number of protons $N \ll Z$, and therefore the repulsion force between p-p has a significant value. The $N \ll Z$ nucleus here is unstable (easy to disintegrate).
- ✓ Since we have undetermined states, we use the mirror nuclei's states to confirm them. In addition, the shell model calculations are primordial in the comparison.
 - Note that the PSDPF interaction is an isospin independent and Coulomb free, so it gives the same results for mirror nuclei.

We present on **Table III-1**, the energy spectra, of the mirror nuclei ^{22}Si and ^{22}O [10]. Since the ^{22}Si is deficient of neutrons, it was difficult to study it experimentally, we show on the table the theoretical results obtained in Ref. [44] using the Gamow shell model (GSM). Concerning the mirror ^{22}O , only the first excited state with $J^\pi = 2^+$ was well identified and all the other states have uncertain J^π and needs to be confirmed using shell model calculation.

The ^{24}Si case

^{24}Si		^{24}Ne	
E level (MeV)	J^π	E level (MeV)	J^π
0.0	0^+	0.0	0^+
1.879	2^+	1.981	2^+
3.449	$(2^+)^*$	3.868	2^+
3.471	$(4^+, 0^+)^*$	3.972	4^+
		4.766	0^+
		4.880	
		5.575	2^+

Table III-2: Comparison of the first excited states in the mirror nuclei ^{24}Si and ^{24}Ne [10],

* States taken from Ref. [45].

On **Table III-2**, are presented the excitation energy spectra of the mirrors ^{24}Si and ^{24}Ne [10, 45]. We remark that the ^{24}Si has 3 observed excited states [45], 2 of them have uncertain J^π assignments. Like the usual mirror nuclei, the ^{24}Ne has more excited states with well-known J^π except for the 4880 keV state. No negative parity states were identified in both mirrors.

The ^{26}Si case

^{26}Si		^{26}Mg	
E level (MeV)	J^π	E level (MeV)	J^π
0.0	0^+	0.0	0^+
1.797	2^+	1.808	2^+
2.787	2^+	2.938	2^+
3.336	0^+	3.082	
3.757	(3^+)	3.420	
3.842	(4^+)	3.564	
4.139	2^+	3.588	0^+
4.187	(3^+)	3.941	3^+
4.446	(4^+)	4.318	4^+
4.796	(4^+)	4.332	2^+
4.811	(2^+)	4.350	3^+
4.831	0^+	4.644	
5.147	2^+	4.835	2^+
5.229	(2^+)	4.901	4^+
5.289	4^+	4.972	0^+
5.517	(4^+)	5.180	
5.676	1^+	5.291	2^+
5.890	0^+	5.476	4^+

5.929	3^+	5.691	(1^+)
5.945	(0^+)	5.711	$(1^+, 2^+)$
6.101		5.715	4^+
6.295	2^+	6.125	3^+
6.382	(2^+)	6.256	0^+
6.461	0^+	6.483	
6.765		6.622	(4^+)
6.787	3^-	6.634	
6.810		6.745	2^+
6.880	(0^+)	6.876	3^-
7.018	(3^+)	6.951	
7.154	2^+	6.971	(4^+)
7.198	(5^+)	6.978	(5^+)
7.418	(4^+)	7.061	1^-
7.496	2^+	7.099	2^+
7.522	(5^-)	7.002	$(0, 1)^+$
7.606		7.264	3^+
7.674	(2^+)	7.261	
7.701	(3^-)	7.282	(4^-)
7.886	(1^-)	7.348	3^-
7.921		7.371	2^+

Table III-3: Comparison of the first excited states in the mirror nuclei ^{26}Si and ^{26}Mg [10].

The energy spectra of the $A = 26$ are represented on **Table III-3**, there are more available states in ^{26}Si and the mirror ^{26}Mg with some unknown J^π . In ^{26}Si there, are three proposed negative parity states contrary to its mirror that has three confirmed ones.

The ^{28}Si case

^{28}Si	
E level (MeV)	J^π
0.0	0^+
1.779	2^+
4.617	4^+
4.979	0^+
6.276	3^+
6.690	0^+
6.878	3^-
6.887	4^+
7.380	2^+
7.416	2^+
7.799	3^+
7.933	2^+
8.258	$2^{(+)}$
8.328	1^+
8.413	4^-
8.543	6^+
8.588	3^+
8.819	
8.904	1^-
8.945	5^+
8.953	$(0^+, 1, 2)$
9.164	(4^+)
9.315	3^+

9.381	2 ⁺
9.417	4 ⁺
9.479	(2 ⁺)
9.496	(1 ⁺)
9.702	(5 ⁻)
9.764	(3 ⁻)

Table III-4: Experimental review of the first excited states in ²⁸Si [10].

On **Table III-4**, is shown the energy spectrum of ²⁸Si, which has well studied states but some of them have uncertain J^π that need to assigned. Three possible negative parity states were identified.

The ³⁰Si case

³⁰ Si	
E level (MeV)	J^π
0.0	0 ⁺
2.235	2 ⁺
3.498	2 ⁺
3.769	1 ⁺
3.787	0 ⁺
4.810	2 ⁺
4.830	3 ⁺
5.231	3 ⁺
5.279	4 ⁺
5.372	0 ⁺
5.487	3 ⁻
5.614	2 ⁺

5.950	4 ⁺
6.503	4 ⁻
6.537	2 ⁺
6.641	2 ⁻
6.642	0 ⁺
6.744	1 ⁻
6.865	3 ⁺
6.914	(2 ⁺)
6.998	5 ⁺
7.043	5 ⁻

Table III-5 : Experimental review of the first excited states in ³⁰Si [10].

The energy spectrum of ³⁰Si up to 7 MeV is shown on **Table III-5**. We note here, that almost all the excited states are certain with well-defined J^π ; five of them have negative parity.

The ³²Si case

³² Si	
E level (MeV)	J^π
0.0	0 ⁺
1.941	2 ⁺
4.230	2 ⁺
4.983	0 ⁺
5.220	(1 ⁺)
5.288	3 ⁻
5.412	1 ⁺

5.427	2^+
5.502	$(4^+, 5^-)$
5.581	(5^-)
5.773	$(1, 2, 3)$
5.785	$(0, 1, 2)^+$
5.893	(3^+)
5.954	(2^+)
5.967	3^-
6.170	(2^+)
6.195	1^-

Table III-6: Experimental review of the first excited states in ^{32}Si [10].

On **Table III-6**, is presented the energy spectrum of ^{32}Si up to 6 MeV. One can see that most states here have unconfirmed J^π . This spectrum contains nine positive parity states; two of them are uncertain, and eight negative parity states, four of them are uncertain.

The ^{34}Si case

^{34}Si	
E level (MeV)	J^π
0.0	0^+
3.327	2^+
3.590	
4.265	(3^-)
4.380	(3^-)
4.520	
4.971	$(3^-, 4^-, 5^-)$
5.042	

5.330	2 ⁺
6.023	

Table III-7: Experimental review of the first excited states in ³⁴Si [10].

The energy spectrum of ³⁴Si up to 6 MeV is shown on **Table III-7**. The ³⁴Si states have uncertain or unknown assignments.

3. Systematics of the even-A silicon isotopic chain study

Using the PSDPF interaction and the code NATHAN we calculated the excitation energies of the first 3 positive +and 4 negative- parity common excited states: 2⁺, 3⁺, 4⁺, 1⁻, 3⁻, 4⁻, 5⁻, called test states. The obtained results are shown case by case on **Table III-8**.

J^π	²² Si	²⁴ Si	²⁶ Si	²⁸ Si	³⁰ Si	³² Si	³⁴ Si
2 ⁺	3.219	2.116	1.878	1.892	2.235	2.044	4.380
3 ⁺	4.947	4.927	3.990	6.470	4.787	5.602	5.715
4 ⁺	6.903	4.069	4.397	4.645	5.274	5.589	7.565
1 ⁻	6.820	6.511	6.663	7.227	6.665	5.241	4.876
3 ⁻	6.454	6.490	6.716	7.176	5.773	5.495	4.790
4 ⁻	8.844	8.110	7.899	8.604	6.249	6.502	4.254
5 ⁻	9.999	8.602	8.318	8.767	7.360	5.725	4.839

Table III-8: Calculated excitation energies (in MeV) of the test states even-A silicon isotopes.

3.1 Comparison Calculated versus Experimental excitation energies of the test states

All the results obtained using PSDPF of the comparison between experimental [10] and calculated excitation energies for the test states 2⁺, 3⁺, 4⁺, 1⁻, 3⁻, 4⁻, 5⁻ in the even-A silicon isotopes up to N = 19, are discussed in the following subsections.

The 2^+ state

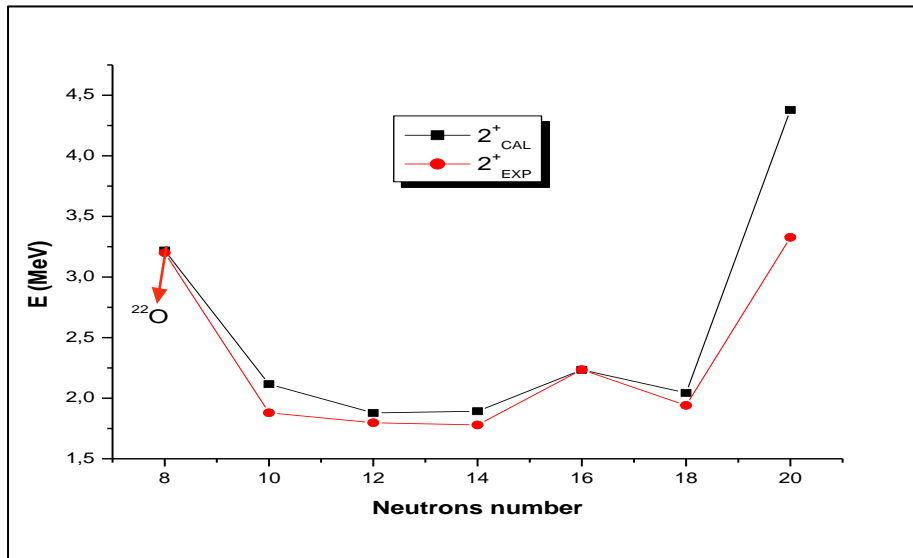


Figure III-2: Comparison between experimental and calculated excitation energies of the 2^+ state in even-A silicon isotopes.

The 2^+ state is known in all the even-A Si isotopes (see Fig III-2), from A=22 to A=34, as a first excited state, an exception is found for ^{22}Si with $N \ll Z$, thus we plotted its mirror state of ^{22}O . This state is located at excitation energies between 1.779 MeV for ^{28}Si and 4.380 MeV for ^{34}Si . The agreement between calculation and experiment is perfect except the case of ^{34}Si . PSDPF predicts the first 2^+ state higher than experiment of 1 MeV in ^{34}Si ($N = 20$), this is expected for a magic nucleus since all the neutron subshells are completely filled.

The 3^+ state

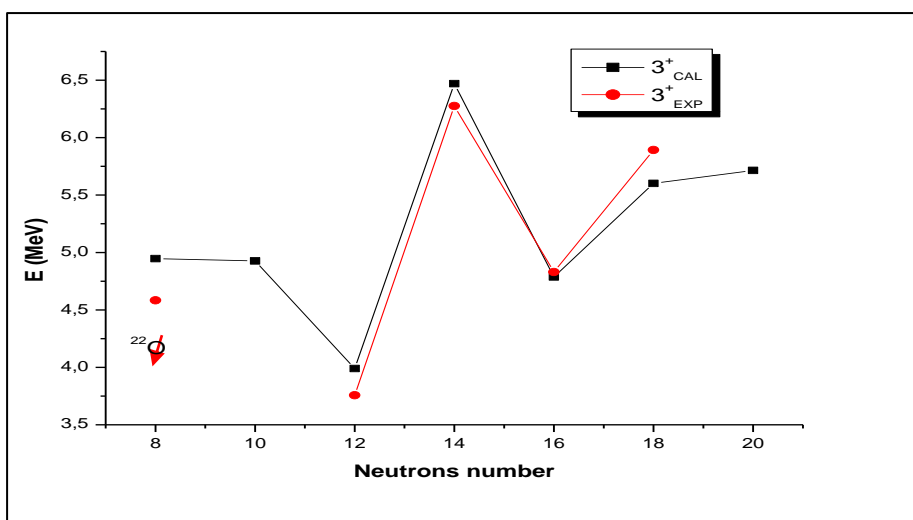


Figure III-3: Comparison between the experimental and calculated excitation energies of the 3^+ in even-A silicon isotopes.

The 3^+ state is known experimentally just in ^{26}Si , ^{28}Si , ^{30}Si , ^{32}Si , we used the 3^+ excitation energy of ^{22}O as shown in Fig III-3. The excitation energies of this state are comprise between 3,757 MeV for ^{26}Si and 6.470 MeV for ^{28}Si . There is an excellent agreement between calculations, using PSDPF, and experiment.

The 4^+ state

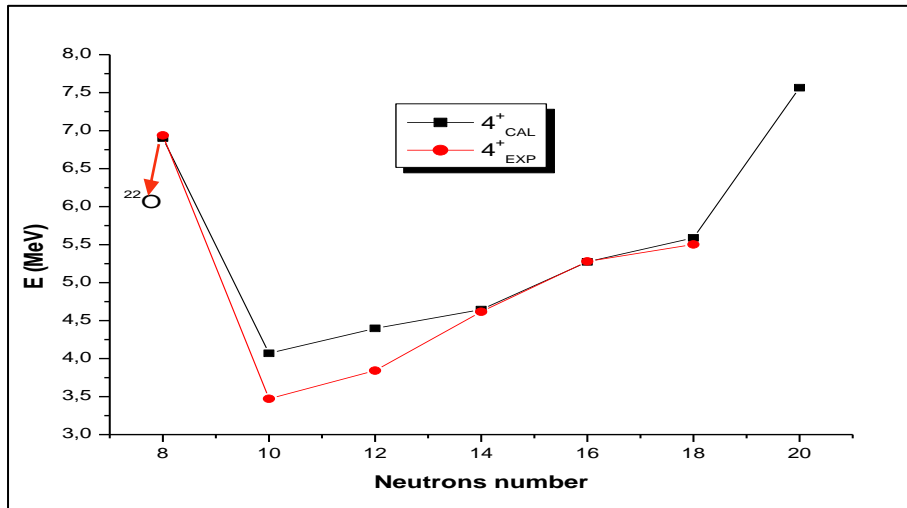


Figure III-4: Comparison between the experimental and calculated excitation energies of the 4^+ in even-A silicon isotopes.

We can see in Fig III-4, that the 4^+ state is known in all the isotopes except in ^{34}Si and ^{22}Si , we used the value of ^{22}O . Its excitation energies vary between 3.471 MeV for ^{24}Si and 7.565 MeV for ^{34}Si . The calculation is in good agreement with experiment.

The 1^- state

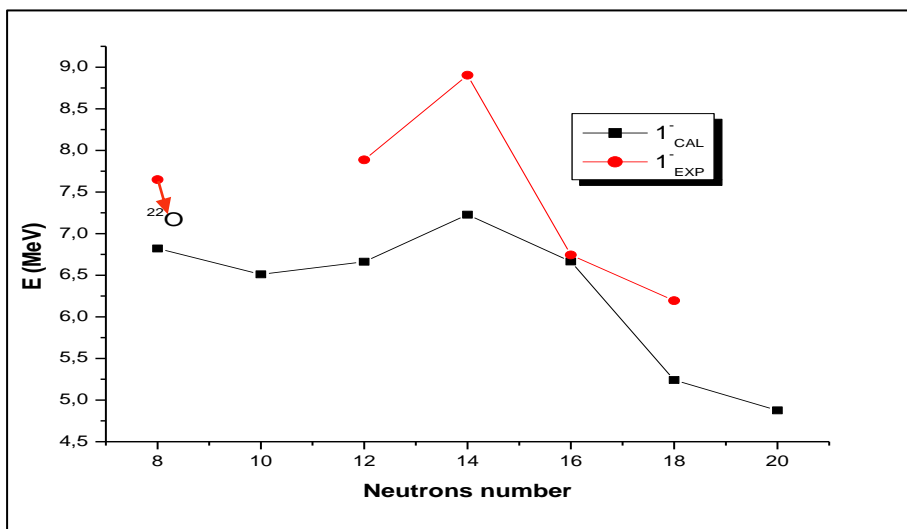


Figure III-5: Comparison between the experimental and calculated excitation energies of the 1^- in even-A silicon isotopes.

We present in Fig III-5 the comparison experimental versus theory of the excitation energies of the 1^- state in even-A silicon isotopes. This observed excitation energies are comprised between 4.876 MeV for ^{34}Si and 8.904 MeV for ^{28}Si . This state is well reproduced by PSDPF only in ^{30}Si . We remind that all these isotopes could not be included in the fit of the PSDPF interaction and we expect such discrepancies.

In order to improve the result of this state, we decided to recalculate; by adding the rmsd (root mean square deviation), which is given by: $\text{rmsd} = \sqrt{\frac{1}{n} \sum_{i=1}^n (E_{\text{cal}} - E_{\text{exp}})^2}$.

The rmsd for the 1^- state equals 1.215 MeV. The new excitation energies are listed on **Table III-9**.

Si	Eexp (MeV)	Ecal (MeV)	ΔE (MeV)	$(\Delta E)^2$ (MeV)	Ecal + rmsd	$\Delta E'$ (MeV)
Si^{22}	7.649	6.82	-0.829	0.687241	8.035	0.386
Si^{26}	7.886	6.663	-1.223	1.495729	7.878	-0.008
Si^{28}	8.904	7.227	-1.677	2.812329	8.442	-0.462
Si^{32}	6.195	5.241	-0.954	0.910116	6.456	0.261
rmsd				1,2150523		

Table III-9: New calculated excitation energies of the 1^- state by adding the rmsd.

The comparison between the experimental and new calculated excitation energies of the 1^- state is shown on Fig III-6. We remark that there is now a quite good agreement experiment versus theory.

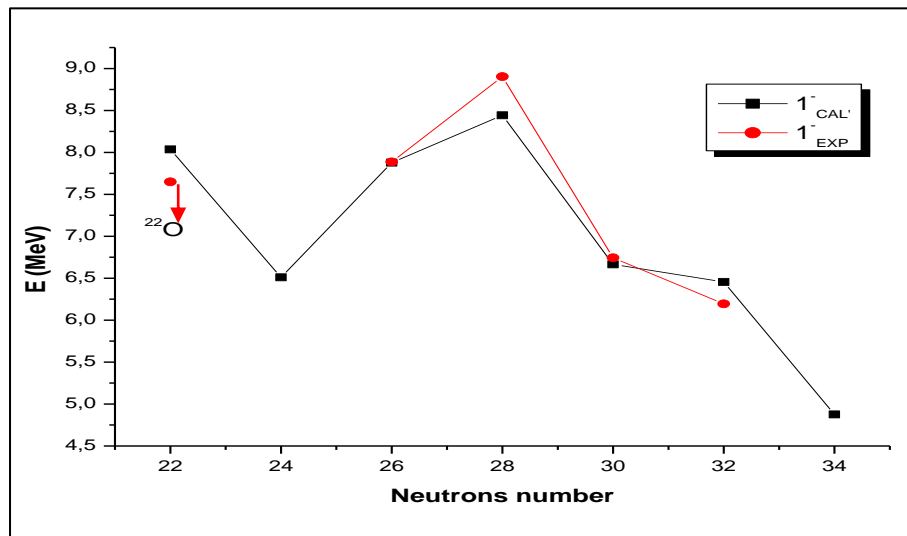


Figure III-6: Comparison between the experimental and the new calculated excitation energies of the 1^- in even-A silicon isotopes.

The 3⁻ state

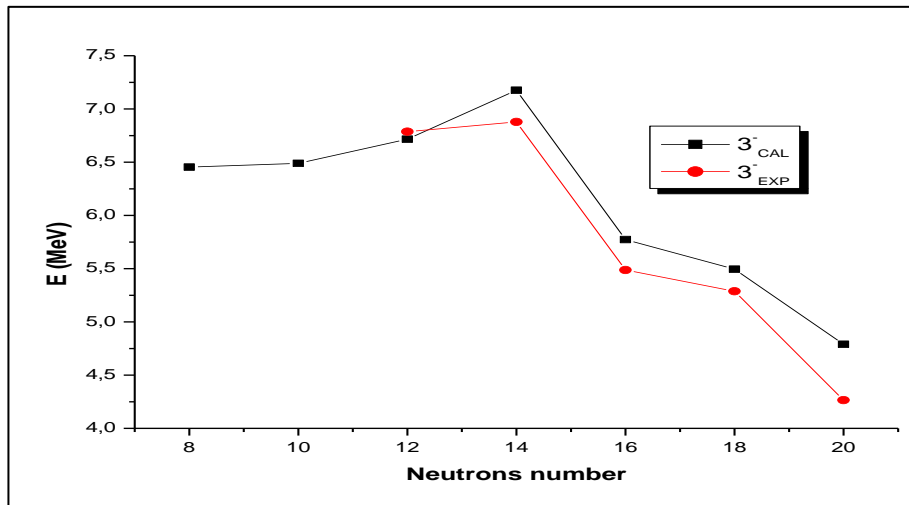


Figure III-7: Comparison between the experimental and calculated excitation energies of the 3⁻ in even-A silicon isotopes.

Figure III-7 that the 3⁻ state is not observed in ²²Si and ²⁴Si. It is located at excitation energies between 4.790 MeV for ³⁴Si and 7.176 MeV for ²⁸Si. The agreement between the observed and calculated excitation energies is quite good.

The 4⁻ state

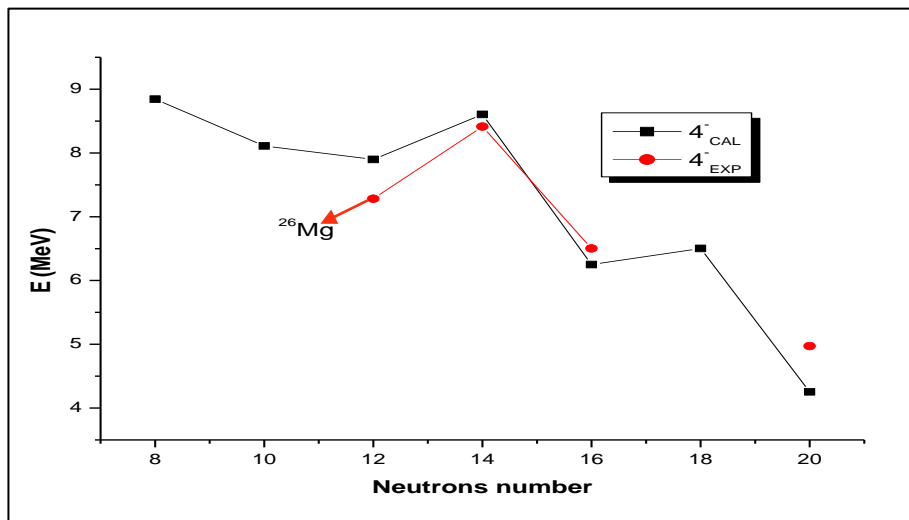


Figure III-8: Comparison between the experimental and calculated excitation energies of the 4⁻ in even-A Silicon isotopes.

The 4⁻ state is less known in the studied isotopes, we used the energy of ²⁶Mg, the mirror of ²⁶Si (see Fig III-8). The observed excitation energies are well reproduced by PSDPF.

The 5⁻ state

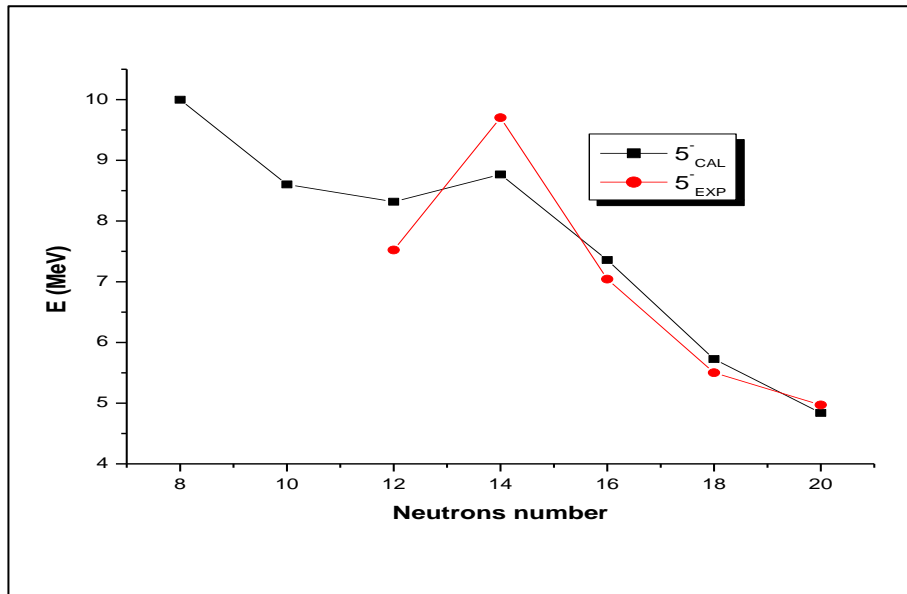


Figure III-9: Comparison between the experimental and calculated excitation energies of the 5⁻ in even-A Silicon isotopes.

The 5⁻ is not observed in ²²Si and ²⁴Si (see Fig III-9), and is comprised between the excitation energies 4.839 MeV for ³⁴Si and 9.999 MeV for ²²Si. The difference between calculated and experimental excitation energies is low for the isotopes at the end of sd shell. While in ²⁶Si and ²⁸Si these differences equal to $\Delta E(^{26}\text{Si}) = 0.796$ MeV, $\Delta E(^{28}\text{Si}) = -0.935$ MeV, respectively. We think that this state has collective configuration (3p-3h) in the case of ²⁸Si, which makes its energy higher than experiment. Such collective states cannot be reproduced using our PSDPF interaction because their configuration is out of the p-sd-pf valence space.

P.S

If the excitation energy is higher than its experimental counterpart; this is explained by the fact that these nuclei are far from closure shells, and that the excitation of a nucleon from the shell p to sd or sd to pf requires a superior energy than for the nuclei at the beginning or the end of the shell.

3.2 Systematics of the excitation energies of the test states in even-A silicon isotopes

In this section we will discuss the evolution of the excitation energies of the test states throughout the even-A Si isotopes. We compared the experimental and calculated, using PSDPF, the excitation energies of the + test states 2⁺, 3⁺, 4⁺ in the previous Figures III-2, III-3, III-4; and listed their values in the Appendix. Further, Figures III-5,6, III-7, III-8, III-9 represent the comparison of excitations energies in the - test states 1⁻, 3⁻, 4⁻, 5⁻. In order to

make our systematic study based on the most probable wave function (Slater determinant) we calculated also, using PSDPF, the shell occupation probabilities, discussed in Chapter II, for all the test states in question. The results are shown, for each state in all the studied isotopes, in Figures III-10 to III-16. The systematic evolution will be discussed state by state.

The 2⁺ state

As shown in the Figure III-2, the variation shape of the 2⁺ states excitation energies is quite well reproduced by the PSDPF interaction. Remind that the first excited state in all the silicon isotopes is the 2⁺, where the ground state in all of them is 0⁺, this is a particular properties of any even-A (even N and Z) nucleus.

As shown in **Figures III-10**, we get the following remarks:

- The 0⁺ ground states correspond to protons full filling the shell $d_{5/2}$ in all the isotopes.
- The 2⁺ states are obtained from the excitations of nucleons within the same sd-shell, and follow the same distribution as the ground state. On the other hand, the closure of the neutron subshells $d_{5/2}$ and $2s_{1/2}$, when approaching the magic N = 20 number, can give rise to reduce the possibility of nucleon arrangement within the sd shell. That can explain the need to more nucleon excitations across the sd-pf shells for ³⁴Si, which is out of our p-sd-pf valence space using the PSDPF interaction for which just one nucleon jump is permitted.

P.S :

- In ²⁸Si the probability of nucleon distribution is always equal between the neutrons and the protons towards $1d_{5/2} \rightarrow 2s_{1/2}$, that is expected since this isotope has N = Z = 14.
- In ³⁴Si, the collective contribution can be found in all the + states, because the p and sd shells are completely full.

The 3⁺ state

The shape of the variation of the 3⁺ states excitation energies predicted by the PSDPF interaction agrees well with the experimental one, as illustrated Figure III-3.

As shown in **Figures III-11**, we get the following remarks:

- These states result mainly from the rearrangement, within the sd shell, of the proton side, in the isotopes with N < Z, ²²Si, ²⁴Si, ²⁶Si. Concerning the N > Z isotopes, ³⁰Si and ³²Si; the neutron distributions contribute also to the configuration of these states.
- For the N = Z, ²⁸Si the excitation $1d_{5/2} \rightarrow 2s_{1/2}$ has the same probability for protons and neutrons.

The 4⁺ state

The variation of the 4⁺ states excitation energies, calculated by PSDPF, follows the same shape as the experimental one; see Figure III-4. **Figures III-12**, illustrate that the 4⁺ states have the same configurations as the 3⁺ states or the ground states.

✚ The 1⁻ state

Despite the disagreement, as shown in the Figure III-5, between experimental and calculated excitation energies of the 1⁻ states; the variation shape of the 1⁻ states is quite well reproduced by the PSDPF interaction. The excitation energies of this state were readjusted and presented on Figure III-6. The negative parity states have a special interest since they result from one nucleon jump across p-sd or sd-pf shells, unlike the positive parity ones which are obtained from the nucleon arrangements within the sd shell. We take a great interest to their shell occupation probabilities to comprehend the evolution of the excitation with the increasing neutron number in the Si even-A isotopes.

Figures III-13 show that:

- In ²²Si, the 1⁻ state results from one *proton* (34%) or *neutron* (15%) jumps from 1p_{1/2} to sd, a pure p-sd configuration (hole in 1p_{1/2}). No nucleon jump to the pf shell.
- In the N < Z isotopes, ²⁴Si, ²⁶Si, the main 1p → sd excitation comes from the *neutron* side (neutron hole in 1p). There is no nucleon excitation to the pf shell; this state has a pure p-sd configuration.
- For ²⁸Si with N = Z, these states result from a *proton* or a *neutron* promotion with equal probabilities, 50% for each type, from 1p_{1/2} to 2s_{1/2}.

For all the rest isotopes with N > Z, these states correspond to a promotion of one *neutron* from sd to the 2p_{3/2} (neutron in pf). No p-sd excitation was found; a pure sd-pf configuration.

✚ The 3⁻ state

The pace of the variation of the 3⁻ state excitation energies predicted by the PSDPF interaction agrees well with the experimental one, as illustrated Figure III-7.

From **Figures III-14**, we get the following observations:

- In the N < Z isotopes, ²²Si, ²⁴Si, ²⁶Si, these states result from the main 1p_{1/2} → sd excitation, which comes from the *neutron* side (neutron hole in 1p_{1/2}). There is no nucleon excitation to the pf shell; it has a pure p-sd configuration.
- For ²⁸Si with N = Z, the 3⁻ state has almost a pure sd → 1f_{7/2} excitation corresponding to a nucleon in pf shell. This excitation comes from a *proton* or a *neutron* promotion with same probability, 50% for each type.
- For the isotopes with N > Z, ³⁰Si, ³²Si, ³⁴Si, these states correspond to one *neutron* jump from sd to the 1f_{7/2} (neutron in pf). No p-sd excitation was found; a pure sd-pf configuration.

✚ The 4⁻ and 5⁻ states

The variation shapes of the 4⁻ and 5⁻ states are quite well reproduced by the PSDPF interaction; see Figures III-8, III-9.

From the shell occupation probabilities of the 4⁻ and 5⁻ states, shown in **Figure III-15, III-16**, one can catch the following comments:

- Only in the $N < Z$ isotope, ^{22}Si , these 4^- and 5^- states have a main excitation resulting from the *neutron* $1p_{1/2} \rightarrow sd$ jump (neutron hole in $1p_{1/2}$). There is no nucleon excitation to the pf shell; these states have a pure p-sd configuration.
- In the $N < Z$ other isotopes, ^{24}Si , ^{26}Si , these states result from promotion of *proton* across the sd-pf shells, mainly to the $1f_{7/2}$. That means these states have a pure sd-pf configuration corresponding to a proton in fp.
- As for the 3^- state in ^{28}Si with $N = Z$, the 4^- and 5^- states have almost a pure $sd \rightarrow pf$ excitation corresponding to a nucleon in pf shell mainly in $1f_{7/2}$. This excitation comes from a *proton* or a *neutron* promotion with same probability, 50% for each type.
- For the isotopes with $N > Z$, ^{30}Si , ^{32}Si , ^{34}Si , these states have similar configuration that corresponds to a one *neutron* jump from sd to the $1f_{7/2}$ (neutron in pf). No p-sd excitation was found, i.e. a pure sd-pf configuration.

The 2^+ state

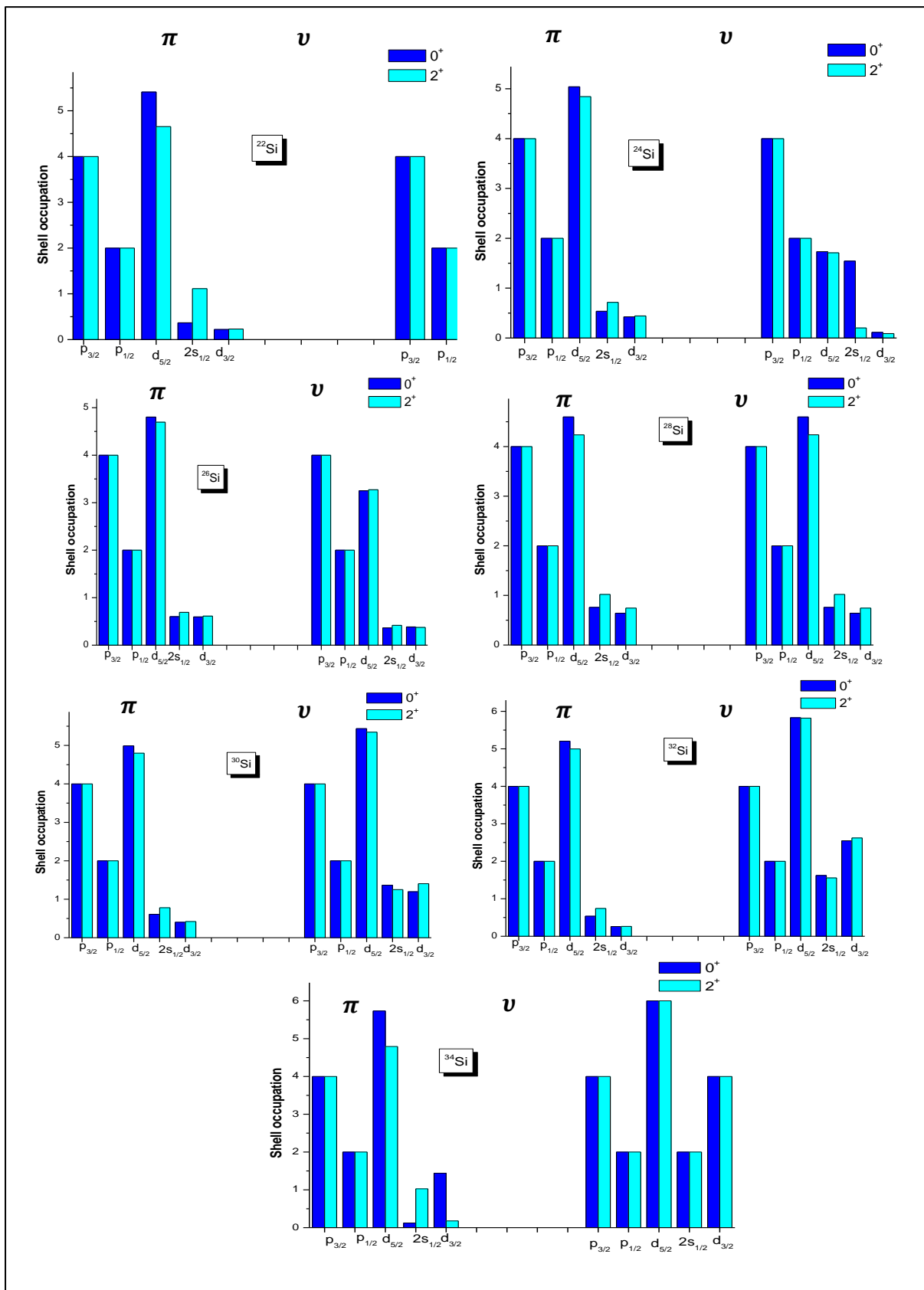


Figure III-10: Shell occupation probabilities of the 2^+ state.

The 3^+ state

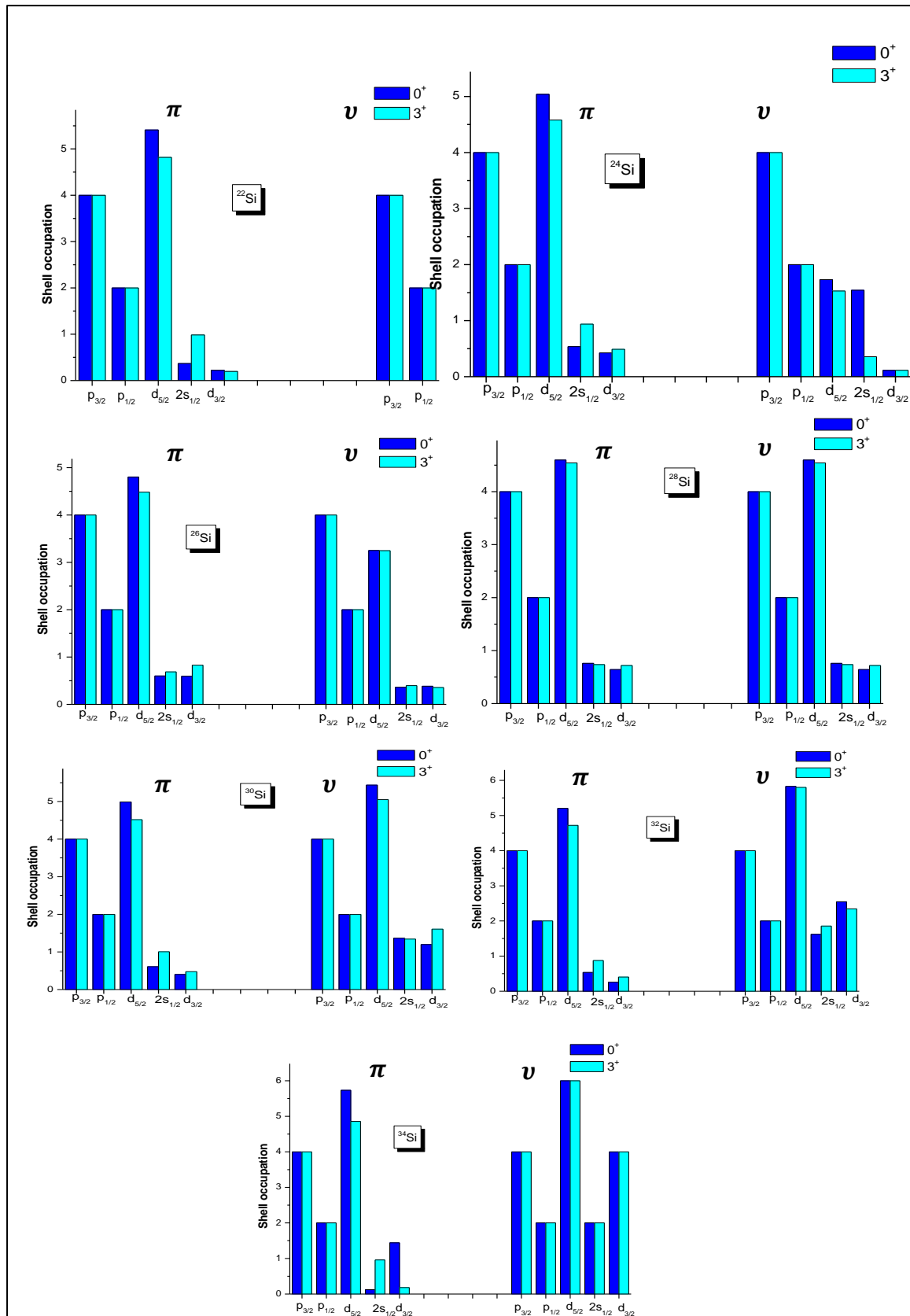


Figure III-11: Shell occupation probabilities of the 3^+ state.

The 4^+ state

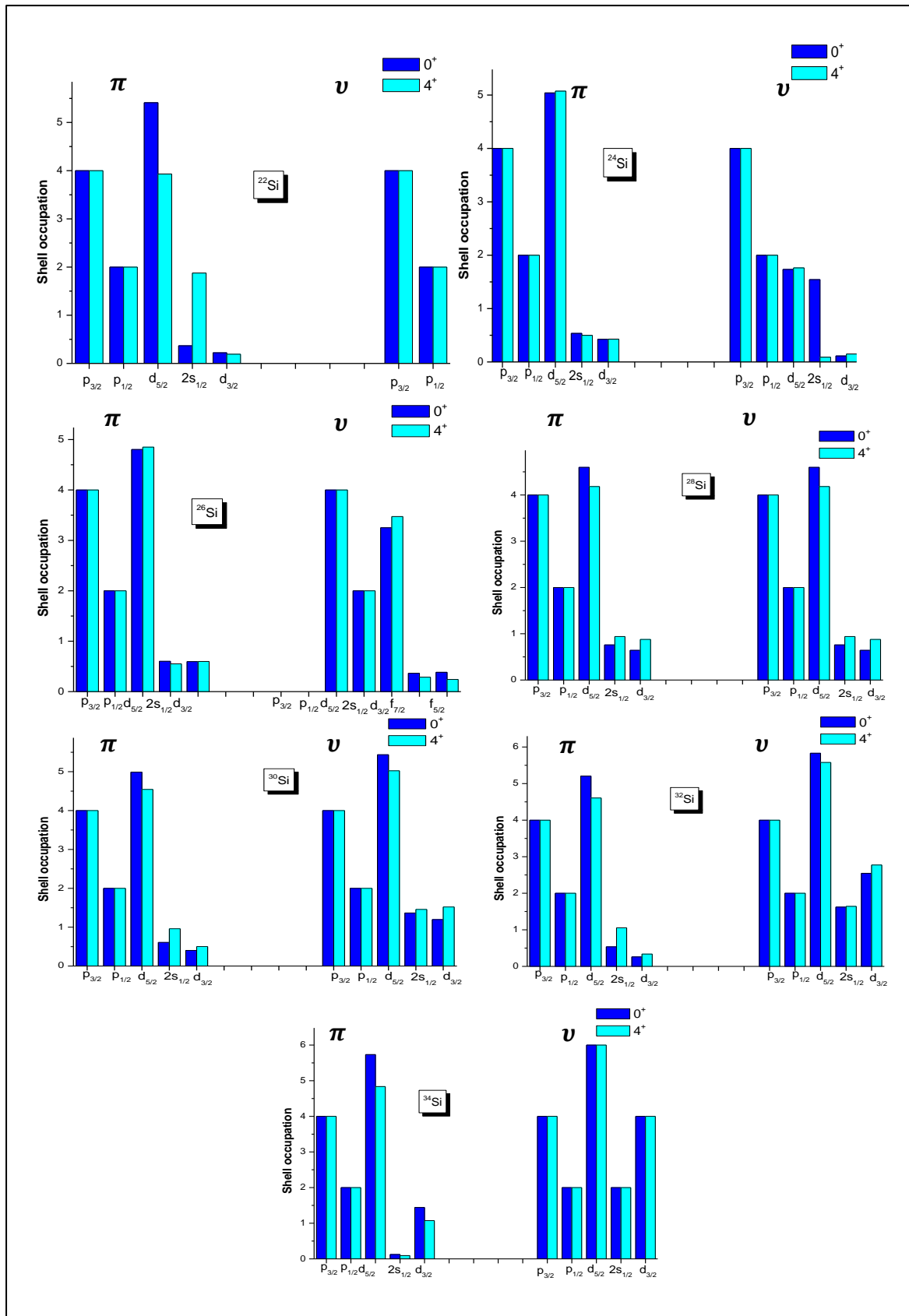


Figure III-12: Shell occupation probabilities of the 4^+ state.

The 1^- state

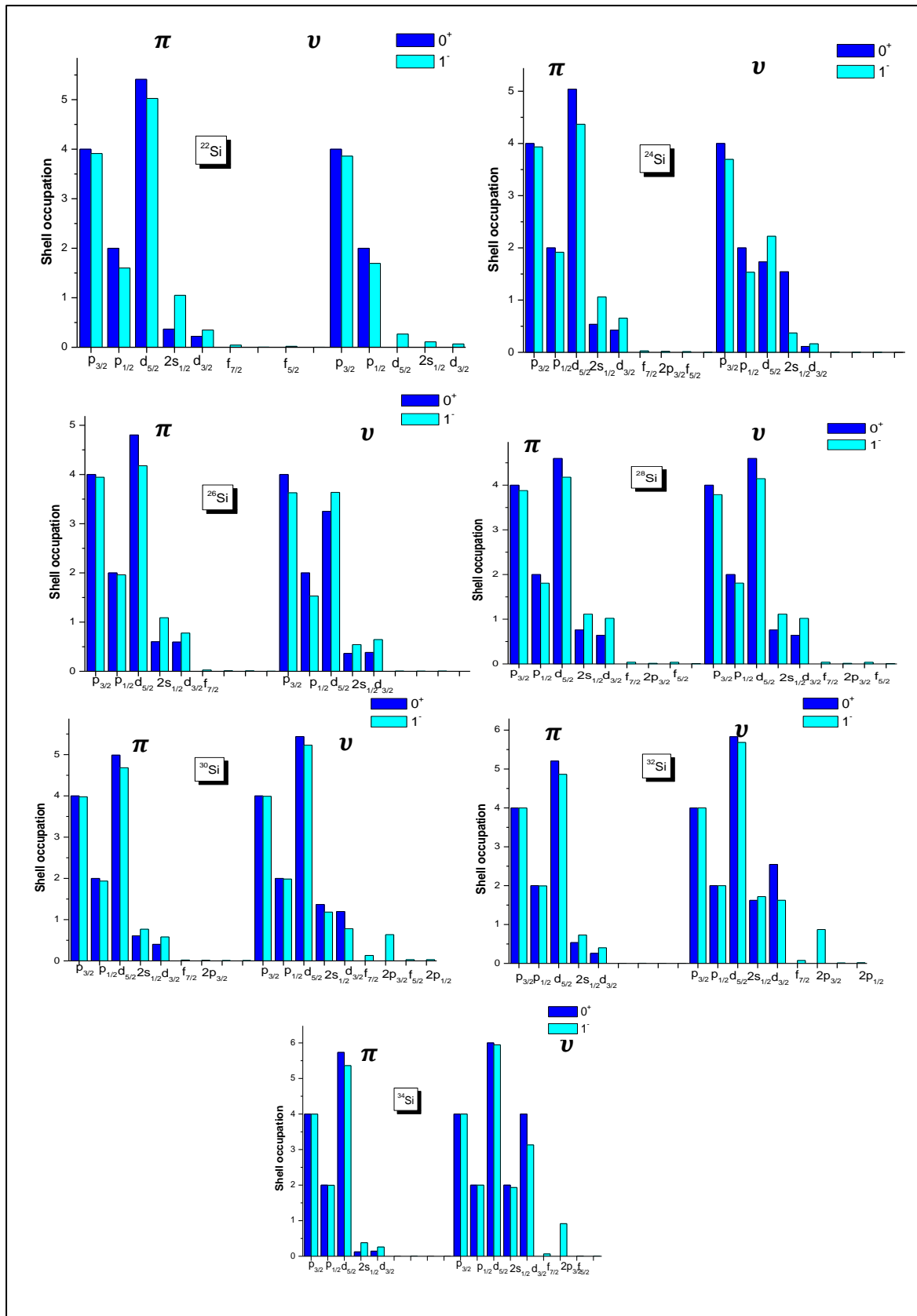


Figure III-13: Shell occupation probabilities of the 1^- state.

The 3^- state

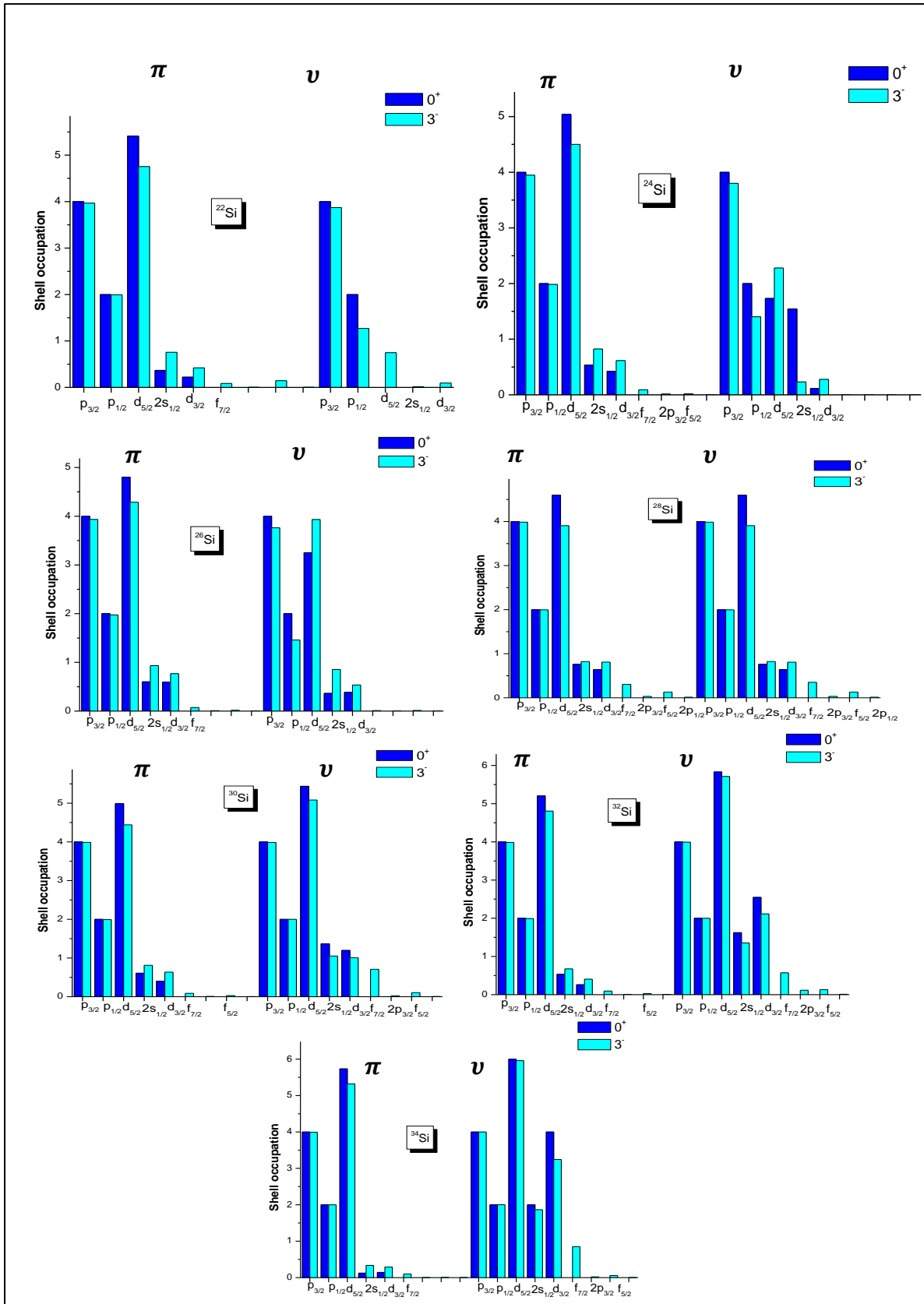


Figure III-14: Shell occupation probabilities of the 3^- state.

The 4⁻ state

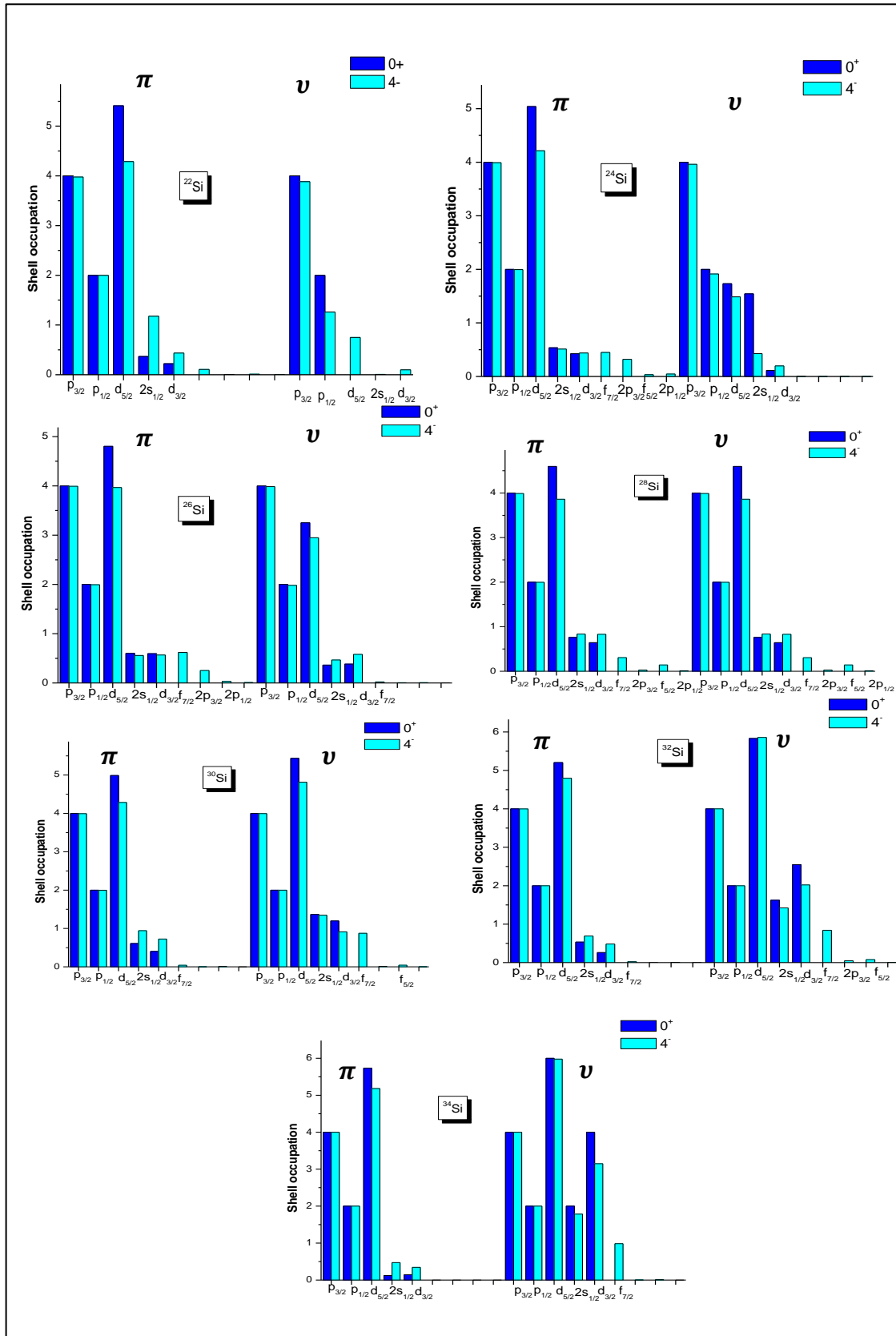


Figure III-15: Shell occupation probabilities of the 4⁻ state.

The 5^- state

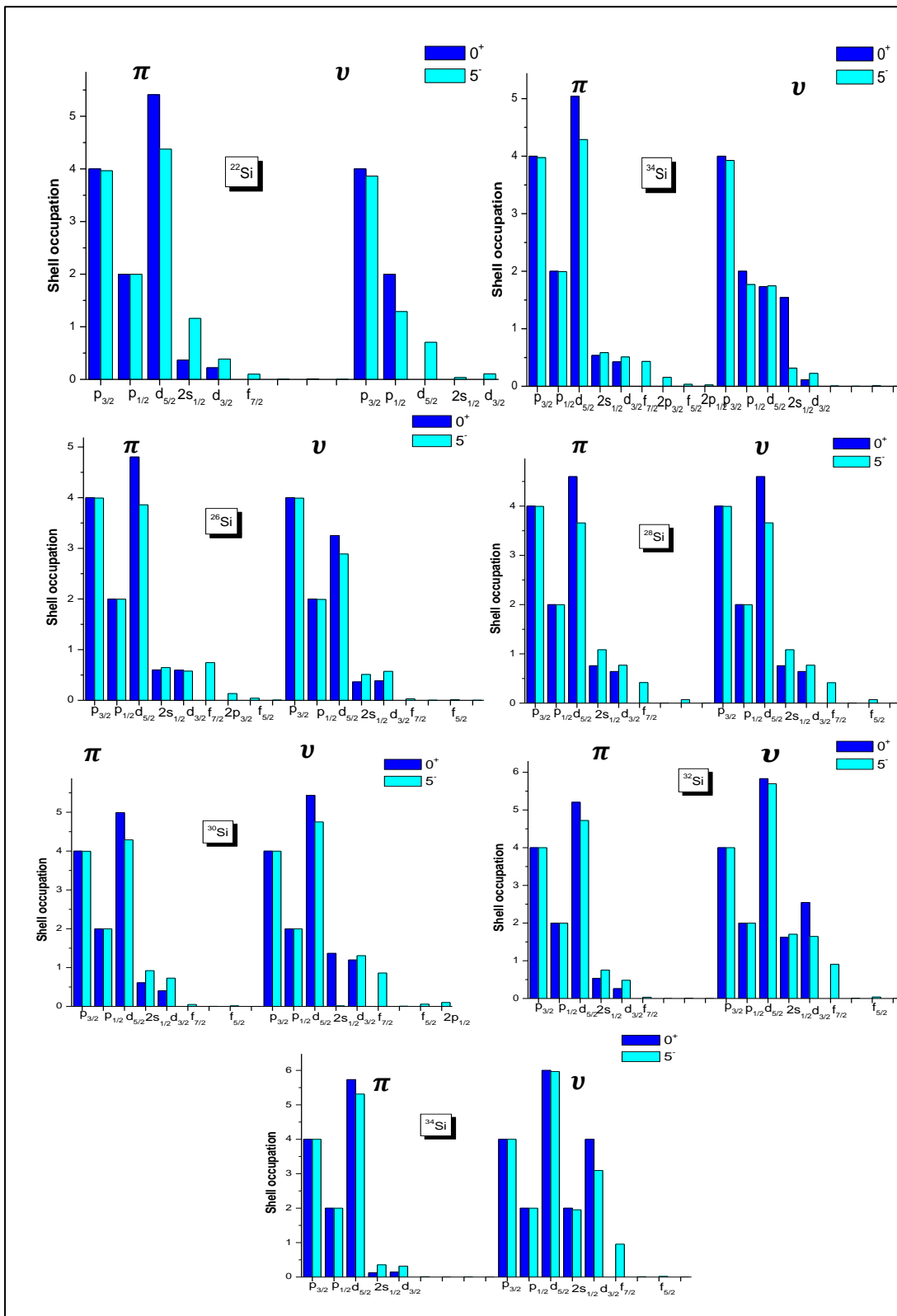


Figure III-16: Shell occupation probabilities of the 5^- state.

Conclusion

We used the PSDPF interaction to calculate the excitation energies of the first + states 2^+ , 3^+ , 4^+ , and – states 2^- , 3^- , 4^- , 5^- in the even-A silicon isotopic chain. Their shell occupation probabilities were also calculated. From this study, we can conclude the following points:

- ❖ The comparison of our results to the observed excitation energies shows a good agreement between experience and theory.
- ❖ This study allowed us to make important predictions of the J^π for isotopes that not only do not have these states but also to have an idea of their energies (see the Appendix).
- ❖ We can note that in the case of the even-A isotopes, the ground state has a $J^\pi = 0^+$.
- ❖ As it is expected, for the isotopes near $N = 8$ closure, the negative parity states result from a hole in p shell. While near $N = 20$ closure, these states result from the promotion of one nucleon to pf shell.

In conclusion, the results of our calculations, discussed in this chapter, have enabled us to demonstrate that the PSDPF interaction very satisfactorily reproduces normal and intruder states in sd-region.

General Conclusion

Our work was devoted to carrying out a systematic study, using PSDPF interaction, of the first + and – excited states in even-A silicon isotopic chain. We focused on even-A silicon (with $A = 22$ to 34), since they are located between in the middle of the sd shell, which could not be included in the fit of the PSDPF interaction.

We used the PSDPF interaction to describe the spectroscopic properties, excitation energy spectra, and wave functions, of the first 0 and $1\hbar\omega$ (+ and –) states of the even-A isotopic chain of silicon. Concerning nuclei with $N < Z$, that are experimentally less studied, we have used the mirror nuclei to determine the J^π of the uncertain or undefined states.

Important predictions have been proposed for each isotope studied. This study allowed us to confirm ambiguous states and to predict spins and/or parities for the indeterminate states in these isotopes, concerning the test states. The obtained results show a good agreement theory versus experiment for the excitation energies of the test states.

This study allowed us to understand the systematic variation of the different + and – test states excitation energies throughout the studied isotopes following their wave function. This gives us an idea of the evolution of the nuclear structure within an isotopic chain. The systematic evolution was well reproduced using the PSDPF interaction.

In conclusion, we can say that the PSDPF interaction successfully described the spectroscopic properties of the studied isotopes; and gives more credit to it.

Bibliographic references

- [1] E. Rutherford, *Philos. Mag*, 6, 21:125, 669 (1911).
- [2] E. Rutherford, *Philos. Mag*, 90:S1, 31 (1919).
- [3] J. Chadwick, *Nature*, 129, 3252, 312 (1932).
- [4] S. Aydin et al., *Phys Rev C* 89, 014310 (2014).
- [5] M. Bouhelal, Ph.D. thesis, under joint supervision of University of Batna, Algeria, and University of Strasbourg, France (2010).
- [6] M. Bouhelal et al., *Nucl. Phys A* 864, 113 (2011).
- [7] M. G. Mayer, *Phys Rev* 75, 1969 (1949).
- [8] O. Axel, J. H. D. Jensen, H. E. Suess, *Phys Rev* 75, 1766 (1949).
- [9] K. S. Krane, “Introductory Nuclear Physics”, Wiley & Sons (1987) pp 67.
- [10] <http://www.nndc.bnl.gov/nudat2>.
- [11] K. E. Johnson, “From Natural History to the Nuclear Shell Model: Chemical Thinking in the Work of Mayer, Haxel, Jensen, and Suess” (2004) pp 296.
- [12] M. Trocheris, *J. Phys. Radium* 13, 299 (1952).
- [13] P. J. Brussaard, P.W.M. Glaudemans, “Shell–Model Applications in Nuclear Spectroscopy”, North–Holland (1977).
- [14] Luc valentin, “Physique subatomique: noyaux et particules”, Hermann (1975).
- [15] A. Bohr and B. Mottelson, “Nuclear Structure”, Vol. 1, Word Scientific (1998) pp 223.
- [16] K. Heyde, “Basic ideas and concepts in nuclear physics”, Institute of Physics Publishing, 2nd edition (1999) pp248.
- [17] A. Vancraeynest, Ph.D. thesis, University of Claude Bernard Lyon-I, France (2010) pp 17.
- [18] J. P. Coffin et al., “Rapport de Prospective : physique corpusculaire”, Vol 1 : Physique Nucleaire, DGRST–Paris (1974) pp 42.
- [19] A. Goasduff, Ph.D. thesis, University of Strasbourg, France (2012).
- [20] E. Caurier, F. Nowacki, *Acta Phys. Pol. B* 30, 705 (1999).
- [21] E. Caurier et al, *Rev. of Mod. Phys.* 77, 427 (2005).
- [22] E. Caurier et al, *Phys Rev C* 59, 2033 (1999).
- [23] R. R. Whitehead, A. Watt, B. J. Cole, I. Morrison, *Adv. Nucl. Phys.* 9, 123 (1977).
- [24] A. Schmidt, *Phys Rev C* 62, 044319 (2000).
- [25] T. Mizusaki, “RIKEN Accelerator Progress Report”, Vol. 33, 15 (2000).
- [26] E. W. Ormand, C. W. Johnson, REDSTICK code, (2002).
- [27] D. Zwarts, *Comp, Phys, Comm.* 38, 365 (1985).
- [28] B. A. Brown, MSU–NSCL Report No. 524 (1985).
- [29] A. Novoselsky, M. Vallières, Drexel University Shell–Model Code DUPSM (1997).
- [30] B. A. Brown, B. H. Wildenthal, *Nucl. Phys A* 474, 290 (1987).
- [31] B. H. Wildenthal, *Prog. Part. Nucl. Phys.* 11, 5 (1984).
- [32] B. A. Brown, W. A. Richter, *Phys Rev C* 74, 034315 (2006).
- [33] W. Heisenberg, *Physics Today* 38, 11, 60 (1985).
- [34] <https://link.springer.com/article/10.12942/lrr-2011-2/tables/2>
- [35] T. Jevremovic, “Nuclear principles in engineering”. 2nd edition, Springer (2009).
- [36] D. Tipping, “Handbook of Stable Isotope Analytical Techniques”. Vol 1, Elsevier B.V. (2004). pp 523
- [37] M. G. Saint-Laurent et al, *Phys Rev Lett* 59,33 (1987).

- [38] J. Äystö et al, Phys Lett B 82(1979) 43.
- [39] E.L. Robinson ,Phys Rev, LP, Purdue, USA, 120,1321 (1960).
- [40] F. W. Aston, Nature 105 (1920) 547.
- [41] R. S. Mulliken, Nature 113 (1924) 423.
- [42] M. Lindner, Phys Rev 91 (1953) 642.
- [43] A. G. Artukh et al, Nucl. Phys. A 176 (1971) 284.
- [44] N. Michel et al, Phys Rev C 100, 064303 (2019).
- [45] C. Wolf et al, Phys Rev Lett 122, 232701 (2019).

Appendix – A

Table contains the experimental and the theoretical values of the excitation energies of the test states in even–A Si isotopes.

	J^π	2 ⁺	3 ⁺	4 ⁺	1 ⁻	3 ⁻	4 ⁻	5 ⁻
The excitation energies								
²² Si	Cal	3.219	4,947	6,903	6,820	6,454	8,844	9,999
	Exp	3.199	4.584	4.75	7.649			
²⁴ Si	Cal	2.116	4,927	4,069	6,511	6,490	8,110	8,602
	Exp	1.879		3.471				
²⁶ Si	Cal	1,878	3,990	4,397	6,663	6,716	7,899	8,318
	Exp	1.797	3.757	3.842	7.886	6.787	7.282	7.522
²⁸ Si	Cal	1,892	6,470	4,645	7,227	7,176	8,604	8,767
	Exp	1.779	6.276	4.617	8.904	6.878	8.413	9.702
³⁰ Si	Cal	2,235	4,787	5,274	6,665	5,773	6,249	7,360
	Exp	2.235	4.830	5.279	6.744	5.487	6.503	7.043
³² Si	Cal	2,044	5,602	5,589	5,241	5,495	6,502	5,725
	Exp	1.941	5.893	5.502	6.195	5.288		6.195
³⁴ Si	Cal	4,380	5,715	7,565	4,876	4,790	4,254	4,839
	Exp	3.327				4.265	4.971	4.971

Table A-1: Experimental versus the theoretical excitation energies values of the test states.

Appendix –B

Tables containing the shell occupation probabilities in even-A silicon isotopes.

²²Si:

For neutrons:

J^π	1p _{3/2}	1p _{1/2}	1p _{5/2}	2s _{1/2}	1d _{3/2}	1f _{7/2}	2p _{3/2}	1f _{5/2}	2p _{1/2}
0 ⁺	4.0	2.0	0.0	0.0	0.0	0.0	0.0	0.0	0.0
2 ⁺	4.0	2.0	0.0	0.0	0.0	0.0	0.0	0.0	0.0
3 ⁺	4.0	2.0	0.0	0.0	0.0	0.0	0.0	0.0	0.0
4 ⁺	4.0	2.0	0.0	0.0	0.0	0.0	0.0	0.0	0.0
1 ⁻	3.864	1.693	0.268	0.110	0.068	0.0	0.0	0.0	0.0
3 ⁻	3.873	1.269	0.748	0.016	0.094	0.0	0.0	0.0	0.0
4 ⁻	3.884	1.262	0.749	0.007	0.098	0.0	0.0	0.0	0.0
5 ⁻	3.864	1.289	0.706	0.036	0.105	0.0	0.0	0.0	0.0

Table B-1: Shell occupation probabilities for neutrons in ²²Si.

For protons :

J^π	1p _{3/2}	1p _{1/2}	1p _{5/2}	2s _{1/2}	1d _{3/2}	1f _{7/2}	2p _{3/2}	1f _{5/2}	2p _{1/2}
0 ⁺	4.0	2.0	5.411	0.368	0.222	0.0	0.0	0.0	0.0
2 ⁺	4.0	2.0	4.655	1.114	0.231	0.0	0.0	0.0	0.0
3 ⁺	4.0	2.0	4.819	0.983	0.197	0.0	0.0	0.0	0.0
4 ⁺	4.0	2.0	3.931	1.877	0.192	0.0	0.0	0.0	0.0
1 ⁻	3.913	1.602	5.025	1.049	0.341	0.0445	0.004	0.020	0.002
3 ⁻	3.968	1.995	4.754	0.756	0.422	0.085	0.003	0.145	0.003

4⁻	3.977	1.999	4.288	1.178	0.436	0.106	0.003	0.012	0.002
5⁻	3.965	1.998	4.376	1.159	0.387	0.100	0.003	0.010	0.001

Table B-2: Shell occupation probabilities for protons in ²²Si.

²⁴Si:

For neutrons:

J^{Π}	1p_{3/2}	1p_{1/2}	1p_{5/2}	2s_{1/2}	1d_{3/2}	1f_{7/2}	2p_{3/2}	1f_{5/2}	2p_{1/2}
0⁺	4.0	2.0	1.733	0.154	0.113	0.0	0.0	0.0	0.0
2⁺	4.0	2.0	1.709	0.202	0.089	0.0	0.0	0.0	0.0
3⁺	4.0	2.0	1.528	0.357	0.115	0.0	0.0	0.0	0.0
4⁺	4.0	2.0	1.763	0.089	0.149	0.0	0.0	0.0	0.0
1⁻	3.695	1.535	2.222	0.371	0.163	0.008	0.003	0.003	0.0
3⁻	3.801	1.402	2.280	0.233	0.278	0.003	0.001	0.003	0.0
4⁻	3.962	1.914	1.487	0.427	0.198	0.006	0.002	0.004	0.002
5⁻	3.926	1.769	1.747	0.316	0.225	0.006	0.001	0.010	0.001

Table B-3: Shell occupation probabilities for neutrons in ²⁴Si.

For protons:

J^{Π}	1p_{3/2}	1p_{1/2}	1p_{5/2}	2s_{1/2}	1d_{3/2}	1f_{7/2}	2p_{3/2}	1f_{5/2}	2p_{1/2}
0⁺	4.0	2.0	5.040	0.536	0.424	0.0	0.0	0.0	0.0
2⁺	4.0	2.0	4.842	0.715	0.443	0.0	0.0	0.0	0.0
3⁺	4.0	2.0	4.580	0.938	0.482	0.0	0.0	0.0	0.0
4⁺	4.0	2.0	5.075	0.498	0.427	0.0	0.0	0.0	0.0
1⁻	3.934	1.917	4.367	1.062	0.655	0.028	0.020	0.014	0.004
3⁻	3.948	1.984	4.500	0.824	0.616	0.090	0.015	0.019	0.004
4⁻	3.991	1.995	4.214	0.512	0.438	0.449	0.321	0.034	0.046

5⁻	3.976	1.994	4.288	0.585	0.510	0.433	0.156	0.035	0.024
----------------------	-------	-------	-------	-------	-------	-------	-------	-------	-------

Table B-4: Shell occupation probabilities for protons in ²⁴Si.

26Si:

For neutrons:

<i>J^π</i>	1p_{3/2}	1p_{1/2}	1p_{5/2}	2s_{1/2}	1d_{3/2}	1f_{7/2}	2p_{3/2}	1f_{5/2}	2p_{1/2}
0⁺	4.0	2.0	3.251	0.365	0.384	0.0	0.0	0.0	0.0
2⁺	4.0	2.0	3.207	0.418	0.374	0.0	0.0	0.0	0.0
3⁺	4.0	2.0	3.247	0.396	0.357	0.0	0.0	0.0	0.0
4⁺	4.0	2.0	3.473	0.286	0.241	0.0	0.0	0.0	0.0
1⁻	3.628	1.531	3.638	0.543	0.646	0.005	0.004	0.005	0.001
3⁻	3.762	1.458	3.632	0.585	0.536	0.010	0.002	0.014	0.001
4⁻	3.986	1.982	2.948	0.467	0.580	0.022	0.005	0.007	0.002
5⁻	3.991	1.992	2.889	0.511	0.572	0.029	0.004	0.012	0.002

Table B-5: Shell occupation probabilities for neutrons in ²⁶Si.

For protons:

<i>J^π</i>	1p_{3/2}	1p_{1/2}	1p_{5/2}	2s_{1/2}	1d_{3/2}	1f_{7/2}	2p_{3/2}	1f_{5/2}	2p_{1/2}
0⁺	4.0	2.0	4.804	0.601	0.595	0.0	0.0	0.0	0.0
2⁺	4.0	2.0	4.696	0.691	0.6134	0.0	0.0	0.0	0.0
3⁺	4.0	2.0	4.483	0.687	0.830	0.0	0.0	0.0	0.0
4⁺	4.0	2.0	4.851	0.551	0.598	0.0	0.0	0.0	0.0
1⁻	3.945	1.962	4.177	1.089	0.778	0.027	0.011	0.011	0.003
3⁻	3.934	1.974	4.287	0.933	0.769	0.073	0.008	0.018	0.004
4⁻	3.992	1.995	3.966	0.559	0.568	0.622	0.253	0.034	0.010
5⁻	3.992	1.998	3.860	0.646	0.576	0.745	0.134	0.043	0.006

Table B-6: Shell occupation probabilities for protons in ²⁶Si.

28Si:

For neutrons:

J^π	1p _{3/2}	1p _{1/2}	1p _{5/2}	2s _{1/2}	1d _{3/2}	1f _{7/2}	2p _{3/2}	1f _{5/2}	2p _{1/2}
0 ⁺	4.0	2.0	4.598	0.760	0.642	0.0	0.0	0.0	0.00
2 ⁺	4.0	2.0	4.236	1.020	0.744	0.0	0.0	0.0	0.0
3 ⁺	4.0	2.0	4.544	0.737	0.720	0.0	0.0	0.0	0.0
4 ⁺	4.0	2.0	4.182	0.940	0.878	0.0	0.0	0.0	0.0
1 ⁻	3.788	1.807	4.177	1.113	1.019	0.037	0.015	0.036	0.007
3 ⁻	3.986	1.996	3.906	0.822	0.809	0.305	0.032	0.131	0.014
4 ⁻	3.990	1.998	3.862	0.834	0.829	0.306	0.027	0.143	0.012
5 ⁻	3.994	1.999	3.660	1.084	0.771	0.415	0.004	0.071	0.002

Table B-7: Shell occupation probabilities for neutrons in ²⁸Si

For protons:

J^π	1p _{3/2}	1p _{1/2}	1p _{5/2}	2s _{1/2}	1d _{3/2}	1f _{7/2}	2p _{3/2}	1f _{5/2}	2p _{1/2}
0 ⁺	4.0	2.0	4.598	0.760	0.642	0.0	0.0	0.0	0.0
2 ⁺	4.0	2.0	4.236	1.020	0.744	0.0	0.0	0.0	0.0
3 ⁺	4.0	2.0	4.544	0.736	0.720	0.0	0.0	0.0	0.0
4 ⁺	4.0	2.0	4.182	0.940	0.878	0.0	0.0	0.0	0.0
1 ⁻	3.788	1.807	4.178	1.113	1.020	0.037	0.015	0.037	0.007
3 ⁻	3.986	1.996	3.906	0.822	0.809	0.305	0.032	0.131	0.014
4 ⁻	3.990	1.998	3.862	0.834	0.829	0.306	0.027	0.143	0.012
5 ⁻	3.994	1.999	3.658	1.084	0.770	0.418	0.004	0.071	0.002

Table B-8: Shell occupation probabilities for protons in ²⁸Si.

30Si:**For neutrons:**

J^π	1p _{3/2}	1p _{1/2}	1p _{5/2}	2s _{1/2}	1d _{3/2}	1f _{7/2}	2p _{3/2}	1f _{5/2}	2p _{1/2}
0 ⁺	4.0	2.0	5.437	1.367	1.196	0.0	0.0	0.0	0.0
2 ⁺	4.0	2.0	5.345	1.251	1.404	0.0	0.0	0.0	0.0
3 ⁺	4.0	2.0	5.052	1.341	1.607	0.0	0.0	0.0	0.0
4 ⁺	4.0	2.0	5.023	1.456	1.520	0.0	0.0	0.0	0.0
1 ⁻	3.989	1.985	5.231	1.184	0.781	0.133	0.636	0.030	0.030
3 ⁻	3.988	1.999	5.081	1.052	1.040	0.703	0.024	0.106	0.007
4 ⁻	3.995	1.200	4.816	1.346	0.913	0.875	0.011	0.0043	0.002
5 ⁻	3.999	1.200	4.752	1.015	1.308	0.860	0.007	0.058	0.002

Table B-9: Shell occupation probabilities for neutrons in ³⁰Si.**For protons:**

J^π	1p _{3/2}	1p _{1/2}	1p _{5/2}	2s _{1/2}	1d _{3/2}	1f _{7/2}	2p _{3/2}	1f _{5/2}	2p _{1/2}
0 ⁺	4.0	2.0	4.990	0.608	0.402	0.0	0.0	0.0	0.0
2 ⁺	4.0	2.0	4.800	0.780	0.421	0.0	0.0	0.0	0.0
3 ⁺	4.0	2.0	4.518	1.006	0.477	0.0	0.0	0.0	0.0
4 ⁺	4.0	2.0	4.543	0.956	0.501	0.0	0.0	0.0	0.0
1 ⁻	3.979	1.934	4.682	0.767	0.580	0.022	0.016	0.010	0.010
3 ⁻	3.988	1.995	4.441	0.810	0.635	0.088	0.008	0.030	0.005
4 ⁻	3.993	1.998	4.286	0.943	0.726	0.042	0.002	0.010	0.001
5 ⁻	3.996	1.999	4.289	0.921	0.728	0.049	0.003	0.014	0.001

Table B-10: Shell occupation probabilities for protons in ³⁰Si.

32Si:**For neutrons:**

J^π	1p _{3/2}	1p _{1/2}	1p _{5/2}	2s _{1/2}	1d _{3/2}	1f _{7/2}	2p _{3/2}	1f _{5/2}	2p _{1/2}
0 ⁺	4.0	2.0	5.831	1.622	2.547	0.0	0.0	0.0	0.0
2 ⁺	4.0	2.0	5.820	1.557	2.623	0.0	0.0	0.0	0.0
3 ⁺	4.0	2.0	5.800	1.855	2.345	0.0	0.0	0.0	0.0
4 ⁺	4.0	2.0	5.578	1.643	2.779	0.0	0.0	0.0	0.0
1 ⁻	3.999	1.998	5.684	1.717	1.624	0.077	0.871	0.013	0.018
3 ⁻	3.992	2.0	5.712	1.354	2.114	0.571	0.116	0.133	0.010
4 ⁻	4.0	2.0	5.88	1.422	2.020	0.842	0.049	0.078	0.001
5 ⁻	4.0	2.0	5.696	1.704	1.645	0.908	0.008	0.038	0.001

Table B-11: Shell occupation probabilities in neutrons in ³²Si.**For protons:**

J^π	1p _{3/2}	1p _{1/2}	1p _{5/2}	2s _{1/2}	1d _{3/2}	1f _{7/2}	2p _{3/2}	1f _{5/2}	2p _{1/2}
0 ⁺	4.0	2.0	5.20	0.535	0.260	0.0	0.0	0.0	0.0
2 ⁺	4.0	2.0	4.996	0.741	0.263	0.0	0.0	0.0	0.0
3 ⁺	4.0	2.0	4.720	0.876	0.404	0.0	0.0	0.0	0.0
4 ⁺	4.0	2.0	4.606	1.056	0.338	0.0	0.0	0.0	0.0
1 ⁻	3.998	1.994	4.865	0.732	0.402	0.001	0.006	0.001	0.003
3 ⁻	3.985	1.993	4.805	0.673	0.405	0.094	0.009	0.029	0.007
4 ⁻	3.998	2.0	4.800	0.692	0.483	0.023	0.001	0.005	0.0
5 ⁻	3.999	2.0	4.721	0.754	0.483	0.034	0.0	0.009	0.0

Table B-12: Shell occupation probabilities for protons in ³²Si.

34Si:**For neutrons:**

J^π	1p _{3/2}	1p _{1/2}	1p _{5/2}	2s _{1/2}	1d _{3/2}	1f _{7/2}	2p _{3/2}	1f _{5/2}	2p _{1/2}
0 ⁺	4.0	2.0	6.0	2.0	4.0	0.0	0.0	0.0	0.0
2 ⁺	4.0	2.0	6.0	2.0	4.0	0.0	0.0	0.0	0.0
3 ⁺	4.0	2.0	6.0	2.0	4.0	0.0	0.0	0.0	0.0
4 ⁺	4.0	2.0	6.0	2.0	4.0	0.0	0.0	0.0	0.0
1 ⁻	4.0	2.0	5.946	1.964	3.132	0.065	0.916	0.006	0.002
3 ⁻	4.0	2.0	5.957	1.865	3.245	0.852	0.020	0.059	0.003
4 ⁻	4.0	2.0	5.979	1.874	3.149	0.983	0.004	0.011	0.0
5 ⁻	4.0	2.0	5.965	1.954	3.096	0.954	0.011	0.019	0.001

Table B-13: Shell occupation probabilities for neutrons in ³⁴Si.**For protons:**

J^π	1p _{3/2}	1p _{1/2}	1p _{5/2}	2s _{1/2}	1d _{3/2}	1f _{7/2}	2p _{3/2}	1f _{5/2}	2p _{1/2}
0 ⁺	4.0	2.0	5.732	0.124	1.443	0.0	0.0	0.0	0.0
2 ⁺	4.0	2.0	4.793	1.028	0.179	0.0	0.0	0.0	0.0
3 ⁺	4.0	2.0	4.859	0.959	0.182	0.0	0.0	0.0	0.0
4 ⁺	4.0	2.0	4.835	0.093	1.073	0.0	0.0	0.0	0.0
1 ⁻	3.998	1.996	5.361	0.380	0.259	0.0	0.004	0.0	0.0
3 ⁻	3.994	1.999	5.321	0.337	0.291	0.050	0.001	0.007	0.002
4 ⁻	4.0	2.0	5.182	0.473	0.344	0.001	0.0	0.0	0.0
5 ⁻	4.0	2.0	5.312	0.357	0.316	0.011	0.0	0.004	0.0

Table B-14: Shell occupation probabilities for protons in ³⁴Si.